第40卷 第1期
2024年3月

华 南 地 质
South China Geology

Vol.40, No.1, 1–27
Mar., 2024

doi:10.3969/j.issn.2097–0013.2024.01.001

沉积再循环碎屑锆石的地质意义及其识别
——以长江流域的碎屑物源研究为例

宋仁龙[1],秦拯纬[2,3*],周光颜[1],鲍　波[2,3]

SONG Ren-Long[1], QIN Zheng-Wei[2,3*], ZHOU Guang-Yan[1], BAO Bo[2,3]

1. 中国地质大学(武汉),湖北 武汉 430074;2.中国地质调查局武汉地质调查中心(中南地质科技创新中心),湖北 武汉 430205;
3. 中国地质调查局花岗岩成岩成矿地质研究中心,湖北 武汉 430205

1. China University of Geosciences, Wuhan 430074, Hubei, China; 2.Wuhan Center of China Geological Survey (Geosciences Innovation Center of Central South China), Wuhan 430205, Hubei, China; 3. Research Center for Petrogenesis and Mineralization of Granitoid Rocks, China Geological Survey, Wuhan 430205, Hubei, China

摘要:碎屑锆石U-Pb年代学分析被广泛应用于限定地层沉积时代、重建沉积物源和古地理格局,结合Lu-Hf-O同位素的分析可以进一步制约地壳生长演化历史。锆石在地表过程中具有极强的稳定性,沉积再循环的碎屑锆石长期以来被认为广泛存在于各类碎屑沉积岩中,对碎屑锆石的数据解读产生重要影响,但是目前还没有简单直接的方式进行有效识别。本文对沉积再循环作用和再循环碎屑锆石判别手段的原理和相关地质应用做了简要总结,包括碎屑矿物结构、岩石化学成分、锆石多同位素年代学分析、多种碎屑副矿物联合示踪和放射性损伤评估等方法,评述了不同方法的优劣和适用条件。本文以长江流域的碎屑物源研究为例,使用源归一化的辐射剂量(α-dose)评估流域内再循环碎屑锆石的存在及其对物源重建的意义。我们强调基于碎屑锆石的研究应该综合区域的沉积记录和岩浆构造历史,考虑沉积再循环作用对数据解读的可能影响,为碎屑锆石数据赋予更加合理的地质解释。

关键词:碎屑锆石;沉积再循环;岩浆构造历史;物源;长江流域

中图分类号:P597　　**文献标识码:**A　　**文章编号:**2097-0013(2024)01-0001-27

Song R L, Qin Z W, Zhou G Y and Bao B. 2024. Geological Significance of the Sedimentary Recycling Detrital Zircon and Its Recognition: Taking Source Study of Clastic Rocks in the Yangtze River Basin as an Example. *South China Geology,* 40(1): 1–27.

Abstract: The U-Pb geochronology analysis of detrital zircons is widely used to constrain the deposit age of strata and reconstruct sediment sources and paleogeographic evolution. Combined with the analysis of Lu-Hf-O isotopes, it can further constrain the history of crustal growth and evolution. Sedimentary recycled detrital zircon is widely present in various types of clastic sedimentary rocks due to its high resistance to surface processes, which has long been considered to bear a significant impact on the interpretation of detrital zircon data. However, there is currently hardly any efficient way to identify sedimentary recycled detrital zircon. This study provides a summary of the principles and related geological applications of sedimentary recy-

收稿日期:2023-10-4;**修回日期:**2023-11-13
基金项目:中国地质调查局地质调查项目(DD20243429、DD20221689)、中国地质调查局花岗岩成岩成矿地质研究中心开放基金课题(PMGR202111)
第一作者:宋仁龙(2000—),男,硕士研究生,地球化学专业,E-mail:rlsong@cug.edu.cn
通讯作者:秦拯纬(1987—),男,高级工程师,从事花岗岩成岩成矿研究工作,E-mail:qinzhengwei@mail.cgs.gov.cn

cling and the discrimination methods for recycled detrital zircons, including means such as detrital mineral structure, rock chemical composition, multi-isotope geochronology analysis on zircons, multiple detrital mineral analysis, and radioactive damage assessment. The advantages and disadvantages of different methods and their applicable conditions have been evaluated. This article presented a case study on zircon provenance in the Yangtze River, using source- normalized radiation α-dose to assess the presence of recycled detrital zircons. We emphasize that research based on detrital zircon should integrate regional sedimentary records and magmatic-tectonic history to provide more reliable geological interpretations for detrital zircon data, considering the potential impact of sedimentary recycling on data interpretation.

Key words: detrital zircon; sedimentary recycling; magmatic-tectonic history; material sources; Yangtze river basin

锆石作为一种副矿物广泛存在于岩浆岩、变质岩和沉积岩中，由于其具有结构稳定、有较强的抗风化和抗蚀变能力等特点，较少受到成岩后的地质作用的干扰而能够完好地保存。锆石含有较高的U、Th和较低的非放射成因Pb，其U-Pb体系封闭温度高达900 ℃，是岩浆岩和变质岩U-Pb年代学研究的理想对象（吴元保和郑永飞，2004）。此外，锆石还可以开展Lu-Hf同位素和O-Si同位素的分析，由于这些元素在锆石中的扩散速率非常低，可以得到可靠的锆石结晶时的同位素组成，为寄主岩石性质和成因提供重要约束。在碎屑沉积岩中，锆石是最常见的重矿物之一，鉴于其在地表风化剥蚀、搬运和沉积成岩等地质过程的稳定性，碎屑锆石可以有效记录物源区母岩的时代和性质，对多颗粒碎屑锆石进行微区测试，并进一步开展统计分析，可以对碎屑沉积岩的沉积时代、物质来源和沉积构造背景等信息提供重要约束（Dickinson and Gehrels, 2008, 2009; Dickinson and Gehrels, 2010; Shaanan and Rosenbaum, 2018）。对现代沉积物中碎屑锆石开展U-Pb-Lu-Hf-O多同位素体系的综合分析，可以限定物源区的地壳生长演化历史（Pietranik et al., 2008; Iizuka et al., 2010, 2013; Yao J L et al., 2012; Dhuime et al., 2012, 2017; Meng L et al., 2015; Zhu Z Y et al., 2023）。随着锆石微区分析技术的发展，碎屑锆石分析方法被广泛应用于沉积学、大地构造学、地球化学等多个学科领域，取得了一系列丰硕的成果（Pell et al., 1997; Hoskin and Ireland, 2000; Wilde et al., 2001; Fedo et al., 2003; Moecher and Samson, 2006; Dickinson and Gehrels, 2009; Voice et al., 2011; Puetz, 2018）。

沉积岩通过风化剥蚀再次进入沉积系统的过程被称为沉积再循环作用。有几点重要的事实或普遍现象，可以说明沉积再循环作用在碎屑沉积系统中普遍存在，并且对碎屑沉积岩的矿物组成和化学成分有重要影响：(1)现代海岸的沉积物、碎屑岩地层，以及逆冲褶皱带中的古老地层，正在或已经发生了大规模的侵蚀风化，产生大量的沉积物进入沉积系统，例如墨西哥湾盆地的西北部大陆架上的沉积物在海退期间发生了大规模的侵蚀，相关河流对三角洲的沉积物输送量高达海退期的数倍（Anderson et al., 2016）；(2)沉积岩和未固结的沉积物占地球表壳面积的大部分(73%~75%)，为现代大陆尺度河流系统提供沉积物（Wilkinson et al., 2009;Peters et al., 2021）。即使在地质历史时期，沉积岩/物的地表占比也不容忽视，与超大陆聚合裂解相关的全球构造活动相关可能会加剧沉积岩的形成和风化（Peters and Husson, 2017）；(3)碎屑沉积岩中经常有一定比例的沉积岩岩屑，例如在砾岩和岩屑砂岩中可以直接观察到沉积岩的碎屑，而一些碎屑矿物的结构和形成时代信息(如碎屑石英和长石残留胶结边、沉积自生矿物碎屑)可以证实该沉积岩中有风化剥蚀的产物，即发生过沉积再循环作用（Basu et al., 2013; Moecher et al., 2019; Dröllner et al., 2023）。

锆石具有极强的物理化学稳定性，相对于其他碎屑矿物，更容易在沉积再循环的过程中保留下来，甚至经历多次沉积再循环作用（Dickinson and Gehrels, 2008; Garzanti et al., 2013a, 2013b; Barham et al., 2021; Andersen et al., 2022）。沉积再循环

锆石被认为普遍存在于碎屑沉积岩中,并且对于碎屑锆石数据的理解有非常重大的影响:(1)碎屑锆石 U-Pb 年代学分析最广泛的应用之一是可以用来限定地层的最大沉积年龄,尤其是对于缺乏化石记录的前寒武纪地层。大陆边缘沉积盆地周缘可能有大量火山活动,其产生的火山物质可以散落到相邻的沉积中心,此时地层中最年轻的碎屑锆石 U-Pb 年龄几乎与地层的沉积年龄相当。通过多颗粒的锆石 U-Pb 年龄测试,获得地层中最年轻的火山锆石结晶年龄,可以限定地层的最大沉积年龄(Dickinson and Gehrels, 2009; Gehrels, 2014)。在汇聚板块边缘的沉积盆地内,俯冲和碰撞背景下的岩浆作用较为强烈,碎屑锆石可能反映同沉积时代的主要年龄峰值(Cawood et al., 2012)。但在离散板块边缘沉积背景下,同时期的中酸性岩浆记录相对较少,以拉张背景下的幔源基性岩浆为主,因此碎屑锆石通常来源于大陆表壳岩石的风化剥蚀。如果沉积岩中存在大量沉积再循环锆石,同沉积时代的火山锆石的信号可能被严重稀释,可能需要大量(large-n)的碎屑锆石 U-Pb 年代学分析才能检索到接近沉积时代的锆石 U-Pb 年龄(Dickinson, 2008; Pullen et al., 2014; Sharman and Malkowski, 2020);(2)碎屑锆石可以记录物源区岩石的时代和性质,通过对沉积岩中多颗粒碎屑锆石 U-Pb 年代学测试,获得碎屑锆石年龄分布的峰值,与可能的源地体主要岩浆作用时代进行比较,可以确定沉积物中碎屑锆石的来源,并限定地层的碎屑物质来源 (Pell et al., 1997; Cawood et al., 2003; Dickinson, 2008; Moecher and Samson, 2006; Gehrels et al., 2009; Dickinson and Gehrels, 2010)。值得注意的是,锆石在地表过程中可以保持其结晶时的 U-Pb-Hf-O 同位素组成,因此碎屑锆石分析揭示的是锆石的初始物源区岩石的时代和性质,而并非直接物源区。如果样品对应的汇水盆地中的沉积岩含有来源于盆地之外的锆石颗粒,并且再循环进入沉积系统,那么基于碎屑锆石的物源分析将出现误判。沉积岩碎屑锆石的年龄组分不一定能代表其汇水盆地内存在该时期的岩浆事件,再循环碎屑锆石的存在对基于碎屑锆石分析的"源-汇系统"重建是一个重大的挑战(Garzanti et al., 2013a; Andersen et al., 2022);(3)地质历史时期的沉积岩和现代沉积物中的碎屑锆石为大面积的大陆地壳提供了代表性样品,是理解大陆地壳的长期生长演化模式的关键材料(Voice et al., 2011; Puetz, 2018)。地球早期的地质体可能在长期的构造活动中被改造或者风化剥蚀,得益于锆石稳定的物理化学特性,这些演化历史可以在碎屑锆石记录中保留。统计大陆尺度或者全球范围的碎屑锆石 U-Pb-Hf-O 同位素数据,是重建大陆地壳生长曲线的重要依据(Pietranik et al., 2008; Dhuime et al., 2012, 2017; Parman, 2015; Roberts and Spencer, 2015)。然而,近年来现代河沙样品中锆石 U-Pb-Lu-Hf 和独居石、磷灰石和榍石 U-Pb-Sm-Nd 同位素分析的研究显示,碎屑锆石所记录的主要地壳生长期次明显更老,与汇水盆地内的岩石记录解耦,而难以在沉积再循环过程中保存下来的其他副矿物则主要记录了较为晚期的地壳生长事件,与岩石记录的统计结果一致(Liu X C et al., 2017; Zhou G Y et al., 2020)。这种差异说明现代河沙中可能存在大量沉积再循环的锆石,这些锆石可能导致基于碎屑锆石记录的地壳生长历史严重偏向早期的事件,使区域大陆地壳生长曲线有显著偏差(Hawkesworth et al., 2009, 2010)。

综上所述,再循环碎屑锆石可能对基于碎屑锆石年代学和同位素分析数据的解读产生巨大影响。但是,这个影响因素在绝大多数目前的研究中还没有被充分评估,最主要的原因在于再循环碎屑锆石往往难以用简单直接的方式识别。锆石在地壳表层的沉积再循环过程中十分稳定,几乎不留下明显的形貌和结构特征,不改变其正常的 U-Pb-Lu-Hf-O 同位素体系,难以与包括岩浆岩和变火成岩在内的结晶基底来源的锆石进行有效区别。前人分别从碎屑矿物结构(Basu et al., 2013)、沉积岩矿物组成和化学成分(Garzanti et al., 2013b)、锆石多种年代学分析(Campbell et al., 2005; Zotto et al., 2020)、多种碎屑矿物联合示踪(Moecher et al., 2019; Barham et al., 2021)以及锆石放射性损伤强度评估等角度来论证沉积再循环物质的影响,鉴别沉积再循环碎屑锆石并评估其对相关地质解释的影响。本文将对以上方法的原理和经典案例做一概述性总结,分析不同方法的优势和适用条件,供今后的研究者

参考。此外，本文系统收集了长江流域基底的岩浆锆石、沉积盖层和主要河流河沙的碎屑锆石 U-Pb 年代学数据，采用源归一化α-dose方法对长江流域干流和支流的碎屑锆石开展分析，探讨再循环碎屑锆石的存在及其对物源示踪的影响。

1 沉积再循环作用和再循环锆石的识别

1.1 沉积岩来源的岩屑/矿物/化石证据

判定沉积再循环的一个最简单、最直接的方法是观察沉积物(岩)中是否出现沉积岩碎屑，例如泥岩、砂岩碎屑等，这些沉积岩来源的碎屑表明沉积物/岩一部分组分至少经历了一次沉积压实成岩和抬升风化剥蚀的再循环过程。沉积岩的压实成岩过程中可能在碎屑矿物之间形成胶结物，或在表面生长沉积自生矿物，例如石英、磷钇矿和独居石(Evans and Zalasiewicz, 1996; Rasmussen et al., 2007)。如果在沉积物的碎屑矿物表面识别到前一世代的残留胶结外皮或者自生边缘，可以作为判别该矿物来自沉积岩的重要证据。然而，由于风化剥蚀和搬运过程中的磨损，这类证据很少能完整保留下来。对于沉积岩而言，确定沉积自生矿物的形成时代需要精细的矿物学和年代学分析工作(Moecher et al., 2019; Dröllner et al., 2023)。

Moecher et al. (2019) 对北美 Appalachian 晚古生代沉积盆地中的碎屑沉积岩中独居石进行了详细的研究，根据独居石的形态特征和年代学结果可以将其分为两类：一类为斑杂状、叶状的独居石或独居石和石英长石的复合晶，Th 含量较低，主要年龄分布在 600~400 Ma；另一类为等轴状、次圆状颗粒，年龄峰值为 1150~1050 Ma。作者认为第一类独居石具有沉积自生或沉积岩低级变质成因的特征，但其 U-Pb 年龄明显早于晚古生代地层的沉积时代，而与该地区的早古生代至晚新元古代地层的沉积时代相对应，代表这些早期沉积岩风化剥蚀的产物。地层中大量存在的太古宙至古元古代碎屑锆石，也可能来自于老的沉积岩的风化剥蚀，综合该地区沉积记录和低温热年代学的证据，部分锆石可能至少经历了五次沉积再循环作用(Zotto et al, 2020; Moecher et al., 2023)。

除了可用于年代学分析的沉积自生矿物，地层中出现明显早于沉积时代的孢粉化石也可以提供沉积再循环的证据(Edwards et al., 2015; Edwards and Pardoe, 2018)。孢粉是陆相地层中最为常见的一类化石，被用作地层划分与对比的化石标志。由于具有稳定且坚硬的外壳，能够较好地保存，有研究证明在河流以及沿海沉积系统中孢粉的运输距离可以达到数百千米(Chmura et al., 1999; Jäger, 2004)。Hadlari et al. (2015) 发现加拿大 Cordillera 造山带的白垩纪地层中存在高达23%的孢粉，为典型的泥盆纪、二叠-三叠纪或侏罗纪化石，明显早于地层的沉积时代，证明这些孢粉化石可能来自于对应时代的碎屑沉积岩的风化剥蚀。结合这些地层中碎屑锆石 U-Pb 年龄分布的相似性，作者认为加拿大 Cordillera 造山带白垩纪地层中存在大量的沉积再循环锆石。

1.2 沉积物成熟度指标

经历过长期沉积搬运或再循环的碎屑矿物不可避免地趋向于较高的成熟度，包括矿物形态与构成组分。在强烈风化剥蚀和搬运等过程中，或压实成岩和再风化剥蚀作用影响下，不稳定碎屑成分(如橄榄石、辉石、角闪石和长石)会较快消耗分解，而较稳定的锆石、金红石和石英等矿物得以保留，矿物形态上为磨圆度较高。随着沉积物成熟度升高，矿物组分的变化也会引起化学组成(如 SiO_2/Al_2O_3)的变化。但是，无论是矿物成熟度还是化学成熟度，不可避免地受到多个因素的控制，对水动力分选、化学风化强度等因素进行排除从而揭示沉积再循环作用是比较困难的。

Shukri (1949) 研究表明：在从尼罗河支流 Atbara 到地中海的运输过程中，沉积物中矿物丰度基本没有改变，即使是橄榄石等不稳定的重矿物也是如此。Kuenen (1959) 通过模拟实验证实了常见造岩矿物(如长石、石英等)在河流运输中的机械磨蚀导致的磨圆度以及粒径的变化可以忽略不计。上述两份研究表明，河流运输中机械磨蚀对矿物成熟度的影响微乎其微，而碎屑颗粒在多次沉积再循环过程中物理磨损的累积效应可能是矿物成熟度升高的原因(Mehring and McBride, 2007)，再循环碎屑锆石通常比第一周期碎屑锆石颗粒磨圆度更

高（Shaanan and Rosenbaum, 2018; Zieger et al., 2019; Zoleikhaei et al., 2022）。但是，地表过程通常更为复杂，不同风化和搬运条件下该方法的有效性还值得检验。变质成因锆石可能具有次圆状或等浑圆状的晶型，火成岩经历变质改造也可能造成部分岩浆成因锆石发生部分溶解而改造其晶体形态，单从锆石形态上鉴别再循环锆石很可能会造成误判。

岩浆过程中 Sc、Th 和 Zr 的元素行为相近，大陆地壳火成岩石中 Zr/Sc 和 Th/Sc 比值沿成分演化线呈正相关关系，而在地表过程中它们同属惰性元素，比值不受化学风化和水动力搬运的影响。在沉积再循环过程中，锆石相对于其他富 Th 的重矿物（如独居石、磷灰石等）更加稳定，再循环碎屑锆石的大量存在导致 Zr/Sc 比值显著增加，从而偏离火成岩演化线（图 1a）。该方法是目前鉴别碎屑沉积岩中是否存在再循环锆石最常用的方法之一。化学风化指数通过计算易迁移元素（K、Na、Ca 和 Mg）与不易迁移的元素 Al 的相对比值，可以反映沉积物中黏土矿物（例如高岭石、蒙脱石、绢云母等）的富集程度。Garzanti et al.（2013b）认为碎屑石英的富集不会显著影响化学蚀变指数 CIA 以及 α^{Al}Na，但是可以导致帕克风化指数 WIP 明显降低（图 1b），

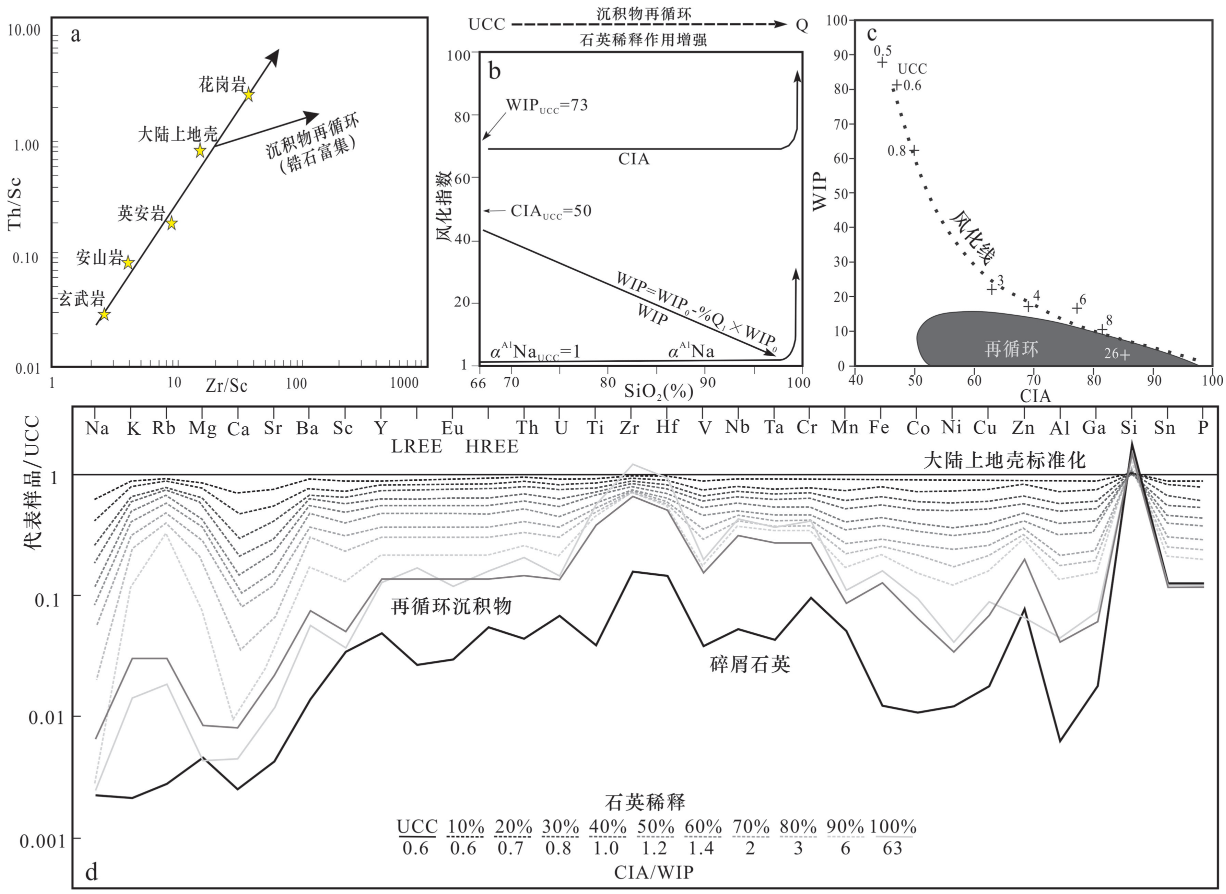

图 1　沉积再循环作用对沉积物地球化学成分的影响

Fig. 1　the effect of sedimentary recycle process on geochemical compositions

a. Th/Sc-Zr/Sc 图解，修改自 Roser and Korsch（1999）；b. CIA、α^{Al}Na 和 WIP 受石英稀释作用的影响情况，修改自 Garzanti et al.（2013b）和 Guo Y L et al.（2018）；c. 使用化学风化指数区分强风化的第一周期与再循环沉积物，再循环沉积物的 WIP 值通常 ≤10，并且 CIA 指数变化范围较大，因此其 CIA/WIP 通常>10，相反，第一周期沉积物 CIA/ WIP 比率相对较低，分布范围一般在 8 以下，并且大部分沿风化线分布. 图中"+"表示采样点与大陆上地壳的平均 CIA/WIP 比率，引自 Garzanti et al.（2013b）；d. 石英砂混入具有大陆上地壳平均成分的碎屑沉积物引起的化学成分变化模拟（灰色虚线），再循环沉积物（灰色实线）和碎屑石英（黑色实线）成分对比，修改自 Garzanti et al.（2013b）

CIA=(Al_2O_3)/(Al_2O_3+CaO*+Na_2O+ K_2O)×100; α^{Al}Na=(Al/Na)$_{sed}$/ (Al/E)$_{UCC}$; WIP=100×(2Na_2O/0.35+MgO/0.9+ 2K_2O/0.25+CaO*/0.7);

UCC-upper continental crust（大陆上地壳）

因此可以联用多个风化指标判断碎屑石英的富集效应，来指示沉积岩风化再剥蚀的产物（图 1c）。此外 Garzanti et al.（2013b）将石英砂混入具有大陆上地壳平均成分的碎屑沉积物中，以模拟沉积过程中随着石英稀释作用的加强，碎屑沉积物化学成分逐渐向再循环沉积物演化的地球化学特征（图 1d），并同时导致碎屑沉积物 CIA/WIP 值逐渐升高，表现出与图 1c 中相似的向再循环组分演化的过程。需要注意的是，相较于密度较小的黏土矿物，密度较大的粒状碎屑矿物（如石英、锆石）沉降速度更快，因此不同风化指标之间的差异可能是水动力分选的结果（Garzanti et al., 2010; Guo Y L et al., 2018）。

1.3 碎屑锆石结合其他矿物联合示踪

由于碎屑锆石具极强的抗机械磨蚀以及化学腐蚀的能力，容易在一次或者多次沉积再循环的过程中保存下来，相较而言，钾长石、独居石、磷灰石、榍石、白云母等矿物更容易在压实成岩、变质作用、再次风化剥蚀和搬运过程中发生分解或磨蚀（Chew et al., 2020）。此外，这些矿物也可以开展年代学（如独居石 U-Th-Pb 定年）和/或同位素（如钾长石 Pb 同位素）分析，提供物源示踪依据（Guo R H et al., 2020; Zhou G Y et al., 2020; Zoleikhaei et al., 2021）。Barham et al.（2021）提出可以通过对比两种稳定性不同的碎屑矿物分别来自结晶基底和沉积岩对沉积岩的贡献比例，来评估沉积再循环作用的强度，以 R 值来度量。

$$R=[(x_1/y_1)/(x_2/y_2)]$$

其中，x、y 分别代表来自结晶基底和沉积岩的物源比例，角标 1 和 2 分别代表稳定矿物相和相对不稳定的矿物相。

如果碎屑矿物全部来自结晶基底，且样品中两种矿物的比例与源岩中矿物丰度的比例相当，得到的 R 值应接近 1，表示碎屑矿物全部来自结晶基底的风化剥蚀。而随着稳定性更强的矿物相的沉积再循环作用增加，R 值将呈指数增长。值得注意的是，各种矿物在不同结晶基底岩石中的丰度可能有非常大的差异（Moecher and Samson, 2006; Samson et al., 2018; Spencer et al., 2018），并且地表风化和沉积搬运过程也会导致不同物性的矿物发生分选（Chew et al., 2020）。因此，联合不同碎屑矿物的物源分析虽然可以揭示更丰富的源区信息，但是两种不同的矿物在矿物成因学、物理化学特性本质上的差异，使得这种对比难以直接评估沉积再循环强度。更可靠的做法是在现代源-汇系统中，将多种碎屑矿物分析与源区岩石信息相结合，并且对比汇区内沉积岩的碎屑锆石信息，结合区域沉积历史和构造隆升历史做综合评判（Moecher et al., 2023）。

1.4 锆石低温热年代学

锆石除 U-Pb 年代学之外，还可以开展（U-Th）/He 热年代学以及锆石裂变径迹等低温热年代学分析。锆石裂变径迹封闭温度为 240±50 ℃（Bernet, 2009），与 U-Th/He 体系的封闭温度相当，明显低于 U-Pb 体系的封闭温度。近年来，碎屑锆石的双定年分析（Double Dating）成为鉴别具有相同 U-Pb 年龄但不同来源碎屑锆石的有效手段，得到了较为广泛的应用（Stevens et al., 2013; Horne et al., 2016; Xu J et al., 2017; Enkelmann et al., 2019）。经历埋藏加热和变质过程的岩石，可能造成其中锆石的低温热年代学和 U-Pb 年代学结果的解耦（Campbell et al., 2005; Reiners et al., 2005）。锆石 U-Pb 年龄和 U-Th/He 年龄之间的差值（ΔT）取决于锆石的结晶寄主岩石性质、抬升剥蚀速率和后期埋藏变质历史。对于快速结晶冷却的火山岩，其岩浆锆石 U-Pb 年龄和 U-Th/He 年龄基本一致，ΔT 在地质年代上可以忽略不计；侵入岩具有相对较慢的冷却抬升速率，其岩浆锆石的 ΔT 相对较大；沉积岩中的锆石在深埋藏和可能的低级变质事件后，都会出现（U-Th）/He 同位素体系的重置，导致该年龄不同程度地小于其结晶年龄。Campbell et al.（2005）在对喜马拉雅造山带锆石的研究中提出可以大致用 $\Delta T \leqslant 300$ Ma 的标准来区分直接由侵入岩剥蚀而来的碎屑锆石和经历过沉积再循环的碎屑锆石，并且认为对于不同的构造热事件，根据需要可以使用不同的值。显然，这一标准在不同地质背景的区域并不通用，需要结合潜在物源区的沉积记录和构造历史多角度论证分析（Zotto et al., 2020）。

1.5 锆石 α 衰变辐射剂量评估

锆石较高的 U、Th 含量导致 α 衰变事件数量（α-dose）的积累，使锆石晶体结构发生晶格错位和晶体损伤。放射性损伤的积累使得锆石晶体逐渐出

现蜕晶化,物理化学稳定性下降,在相同的条件下,较高α-dose的锆石颗粒更加容易在沉积物运输和再循环过程中磨蚀或者分解。因此,通过对比结晶基底锆石和碎屑锆石α-dose,可以揭示这种选择性剔除高α-dose锆石的程度,进而评估锆石是否经历了长距离搬运或再循环过程。

碎屑锆石α-dose计算公式由 Murakami et al.(1991)提出,经 Holland and Gottfried(1955)更正,Dröllner et al.(2022)在后者的基础上进行修改得到:

$$D=8\frac{(X_{\mathrm{U}}\times N_{\mathrm{A}}\times 0.9928)}{(M_{238}\times 10^{3})}\times\left[\exp(\lambda_{238}t)-1\right]$$
$$+7\frac{(X_{\mathrm{U}}\times N_{\mathrm{A}}\times 0.0073)}{(M_{235}\times 10^{3})}\times\left[\exp(\lambda_{235}t)-1\right]$$
$$+6\left(\frac{(X_{\mathrm{Th}}\times N_{\mathrm{A}})}{(M_{232}\times 10^{3})}\right)\times[\exp(\lambda_{232}\,t)-1]$$

D (α-dose)对应于每毫克样品中α衰变的次数(单位:次/mg)。X_{U}和X_{Th}分别代表U和Th浓度(单位: $\times10^{-6}$);t为样品年龄(单位: Ma);N_{A}是阿伏加德罗常数;M_{238}、M_{235}、M_{232}分别为^{238}U、^{235}U、^{232}Th的化学计量数;λ_{238}、λ_{235}和λ_{232}分别是^{238}U、^{235}U和^{232}Th的衰变常数(单位:yr^{-1})。该计算假设^{238}U (c.0.9928)和^{235}U (c.0.0072)同位素的自然丰度基于^{238}U/^{235}U比率为137.88(Steiger and Jäger, 1977)。

通过U、Th含量和锆石结晶年龄计算得到的α-dose值为锆石自结晶之后发生放射性衰变事件次数的理论值,在后期的变质加热过程中锆石可能发生放射性损伤愈合,导致理论上的α-dose值与锆石真实保存的放射性损伤不一致。锆石保存的α-dose积累量可以通过拉曼光谱分析得到。随着放射性损伤的增加,锆石化学键键长和键角发生变化,所有主要拉曼峰强度降低、峰形变宽,并向较低的峰值移动。Nasdala et al.(2001)发现轻度-中度蜕晶化锆石的α-dose积累量与拉曼光谱的主峰半峰宽度呈线性关系,通过测量锆石拉曼光谱,可以反算放射性积累量。值得注意的是,锆石从结晶态到非晶态的转变是可逆过程,加热过程可以使原子在晶格中迁移,位错数量减少,加热淬火后的锆石在冷却时会重新结晶,使锆石蜕晶化区域愈合,恢复晶体结构(Zhang M et al., 2000)。在考虑地质时代的退火时会出现不确定性,Mezger and Krogstad(1997)认为蜕晶化锆石在600~650 °C的条件下可以发生完全重结晶,α-dose归零。拉曼光谱半峰宽得到的α-dose结合U、Th含量可以计算α-dose积累时间,即锆石最后一次加热淬火的时间。与锆石低温热年代学的思路类似,该方法可以得到独立于锆石U-Pb年龄的地质信息,为单颗粒碎屑锆石的来源提供更多制约。

为了判别碎屑锆石与源区岩浆岩锆石的α-dose值差异,Balan et al.(2001)和Dröllner et al.(2022)提出了源归一化α-dose值指标:将碎屑锆石划分为不同的年龄组分,确定对应的岩浆岩源区,将碎屑锆石计算得到的α-dose值与对应岩浆岩中岩浆锆石的α-dose值的比值作为源归一化α-dose值。经历过再循环的锆石或具有长期沉积历史的锆石种群会表现出源归一化α-dose值<1,因为相同年龄相同来源的锆石中,放射性积累较低的颗粒具有更低的蜕晶化程度、更高的物理化学稳定性,因而更容易保存下来。源归一化α-dose值接近1则表示碎屑锆石和源区锆石的α-dose剂量值相似,可能直接来源于岩浆岩的风化剥蚀,没有经历明显的沉积再循环过程。该方法相对于其他方法的优势是锆石的U、Th含量可以在U-Pb年龄测定中同时获得,不需要额外的实验。但是,这一方法最主要的前提是需要确定碎屑锆石的初始来源,因此在现代沉积物中可以得到一定应用,而在地质历史时期沉积岩的物质来源不明确的情况下,需要谨慎看待。同时,蜕晶化锆石在长距离的沉积搬运过程中可能也会损失蜕晶化较严重的组分,影响该方法的有效性。

2 长江流域沉积物中再循环碎屑锆石及其对物源示踪的意义

长江发源于青藏高原东部,注入东海。它是亚洲最长、最大的河流,其流域包含羌塘地块、松潘-甘孜地块、秦岭-大别造山带、华南地块等多个不同构造单元(图2)。华南地块由扬子地块和华夏地块组成,扬子地块占据了长江及其支流近70%的流域面积。上游羌塘地块发育古生代基岩,上覆地层有奥陶系至白垩系(Pullen et al., 2011),而松潘-甘孜

地块则为复理石盆地，其中沉积物的主要来源为秦岭造山带和扬子地块（Weislogel et al., 2006；Enkelmann et al., 2007）。秦岭-大别造山带记录了华北地块和华南地块之间的古生代弧陆碰撞、早中生代陆陆碰撞以及晚中生代碰撞后伸展（Wu Y B and Zheng Y F, 2013）。华南地块由零星出露的太古宙至古元古代结晶基底以及上覆的新元古代至显生宙地层构成，古老的变质结晶主要出露在扬子板块北缘的崆岭（ Zhang S B et al., 2006; Jiao W F et al., 2009; Xiong Q et al., 2009; Gao S et al., 2011;魏君奇和王建雄, 2012; Chen K et al., 2013; Guo J L et al., 2014）、鱼洞子（ 张欣等, 2010; Hui B et al., 2017; Zhou G Y et al., 2018）、钟祥（ Zhang L J et al., 2011; Wang Z J et al., 2013, 2015; Zhou G Y et al., 2015, 2017; Wang K et al.,2018a, 2018b）、陡岭（Hu J et al., 2013; Wu Y B et al., 2014; Nie H et al., 2017）等地区，西南缘的措科（Wang W and Zhou M F, 2014; Wang W et al., 2014）等地区，这些地体的岩石以晚太古代TTG片麻岩和花岗岩以及古元古代花岗质岩石及中高级变质岩为主（Zhao G C and Cawood, 2012; Cawood et al., 2020）。扬子地块的新元古代岩浆岩沿绍兴-江山-萍乡（简称江绍）和东乡-德兴-歙县（也称赣东北）两条构造带广泛分布（舒良树和周国庆, 1988; 周国庆等, 1989; Guo L Z et al., 1989; Wang D Z et al., 1989; Chen J F et al., 1991; Li X H et al., 1994, 2003; 刘伯根等, 1995; 舒良树等, 1995; Shu L S and Charvet, 1996; Zhou G Q and Zou H B, 1996; Li X H, 1999; 吴荣新等, 2005; 曾雯等, 2005; 钟玉芳, 2005; 王孝磊, 2006; Ye M F et al., 2007; Gao J et al., 2009; Shu L S et al., 2011），江南地区东段出露岛弧岩浆岩以及华夏地块东南缘新元古代晚期镁铁-超镁铁岩（Li W X et al., 2005; Wang X L et al., 2006; Shu L S et al., 2006, 2008a, 2008b, 2011; Li X H et al., 2009）。

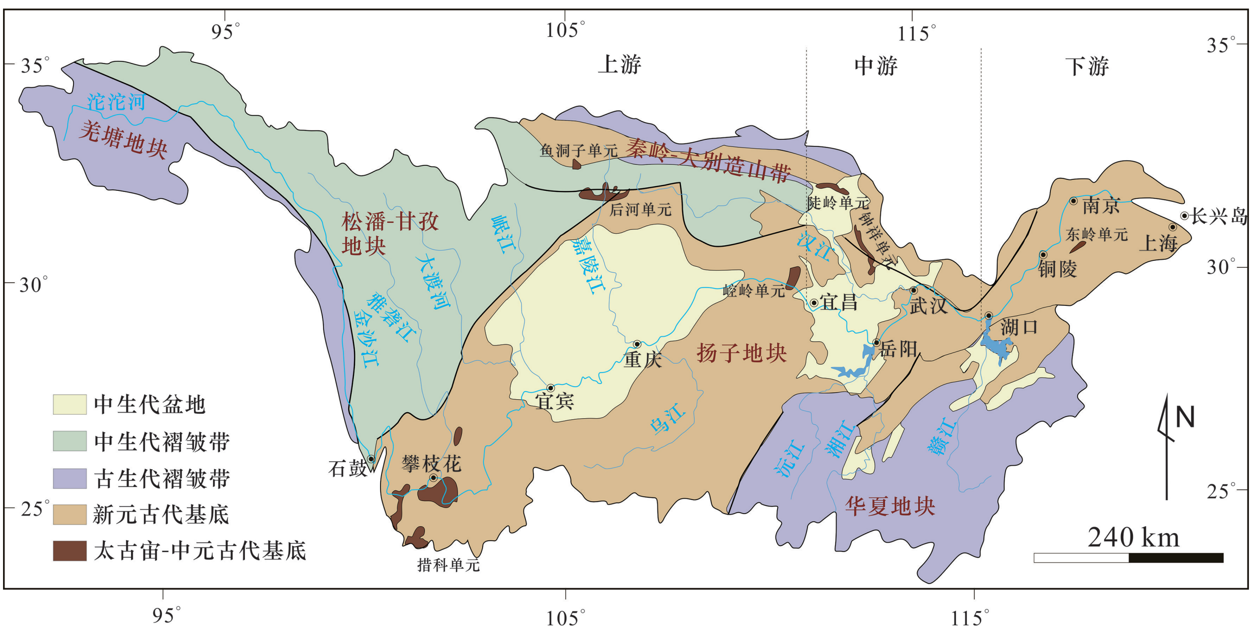

图 2 长江流域构造单元简图

Fig. 2 Schematic map of geological units of the Yangtze River Basin

长江流域覆盖了上述复杂地质单元，自西向东众多的支流汇入干流，且流域内呈现西高东低的地理格局。前人对长江流域的碎屑锆石记录开展了大量的研究，通过锆石形态学和U-Pb年代学分析对长江不同流域的碎屑物质来源进行了详细分析，结合锆石U-Pb年龄和Lu-Hf同位素数据，对华南地

块的地壳生长和演化历史进行重建。但是关于长江流域的沉积来源还存在较大争议。He M Y et al.(2014)对比了长江干流与主要支流河沙中碎屑锆石 U-Pb 年龄图谱的差异,认为长江中上游流域的支流是向长江干流提供砂质沉积物的重要源区,包括汉江、湘江、嘉陵江以及攀枝花与宜宾之间的金沙江干流区域。而碎屑钾长石 Pb 同位素和石英 Be 同位素的研究则发现,长江中游河沙中的碎屑钾长石有约 50%颗粒具有非放射成因的铅同位素,与上游支流中的碎屑钾长石 Pb 同位素一致,而中下游的支流对干流的物质贡献则不明显。Wissink and Hoke(2016)对长江流域的碎屑锆石年龄分布进行定量相似性对比和锆石来源量化模拟,发现长江干流样品碎屑锆石的 U-Pb 年龄分布和物源比例具有高度相似性,并且与上游的雅砻江、岷江、大渡河和嘉陵江等支流的碎屑锆石记录相似,因此认为长江干流的碎屑锆石主要来源于青藏高原东部边缘。

长江流域沉积物和流域内沉积岩盖层的碎屑锆石主要年龄峰值与基底的主要岩浆作用时代一致。值得注意的是,虽然流域内古老结晶基底的出露十分有限,但是碎屑锆石年龄谱中存在明显的 2900~1800 Ma 的峰值,这一年龄组的占比与对应时代的岩石出露面积明显不匹配,特别是在缺乏太古宙至古元古代岩石记录的长江干流和部分支流的沉积物中,2900~1800 Ma 的碎屑锆石年龄组分都以相似的比例存在(图 3)。此外,Liu X C et al.(2017)通过对长江和汉江沉积物的碎屑锆石和独居石对比研究,发现在同一样品中碎屑锆石记录了更高比例的太古宙至古元古代年龄信息,而独居石的记录与流域内的显生宙造山作用历史相匹配,考虑到在沉积再循环过程中锆石相对于独居石的矿物稳定性更强,这两种碎屑矿物记录可能不同程度地受到了再循环碎屑的影响。华南板块广泛分布的新元古代至显生宙的巨厚沉积地层中记录了显著

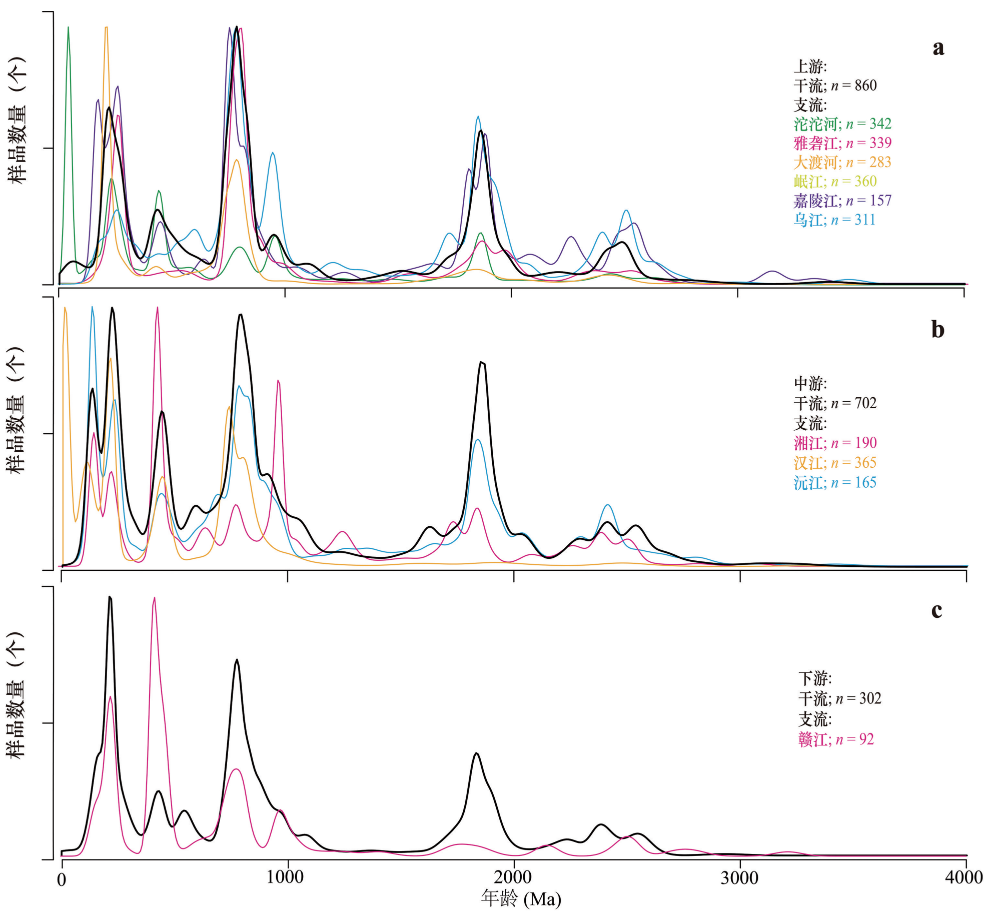

图 3　长江流域现代河流沉积物碎屑锆石年龄谱

Fig. 3　Detrital zircon U-Pb age spectra of modern river sediments in the Yangtze River Basin

的太古宙至古元古代的碎屑锆石U-Pb年龄峰值信息（Wang W et al., 2010; Yang C et al., 2015; Yang Z N et al.,2018; Gan C S et al., 2023），这些沉积岩的风化剥蚀，可能为流域现代沉积物提供大量的再循环锆石。为了验证这一推测，本文系统收集了长江流域内基底岩石中岩浆锆石和沉积盖层中碎屑锆石，以及长江干流及主要支流河沙的碎屑锆石U-Pb年龄数据，计算了不同时代的这三类锆石的α-dose值，采用源归一化法评估长江流域内再循环锆石的存在，讨论其对碎屑锆石数据解读的影响。通过收集整理前人的数据并取其中谐和度大于90%的数据进行后续计算，数据来源见表1。

表1 长江流域现代河流沉积物、沉积盖层及对应结晶基底锆石U–Pb年龄数据来源

Table 1 Summary of zircon U–Pb ages of modern river sediments, related sedimentary rocks, and magmatic zircons from crystalline basement in the Yangtze River drainage basin

长江流域河沙（n=59）				
样品号	采样位置	岩性	分析方法	参考文献
CJ9-3	宜宾	河沙	LA-ICP-MS	Yang S Y et al., 2012
CJ18-1	重庆	河沙	LA-ICP-MS	Yang S Y et al., 2012
04CJ13	宜昌	河沙	LA-ICP-MS	Yang S Y et al., 2012
CJ27	铜陵	河沙	LA-ICP-MS	Yang S Y et al., 2012
CJ1-2	金沙江	河沙	LA-ICP-MS	Yang S Y et al., 2012
CJ1-1	金沙江	河沙	LA-ICP-MS	Yang S Y et al., 2012
CJ3-2	金沙江	河沙	LA-ICP-MS	Yang S Y et al., 2012
CJ6-1	金沙江	河沙	LA-ICP-MS	Yang S Y et al., 2012
CJ6-2	金沙江	河沙	LA-ICP-MS	Yang S Y et al., 2012
CJ4-2	雅砻江	河沙	LA-ICP-MS	Yang S Y et al., 2012
CJ4-3	雅砻江	河沙	LA-ICP-MS	Yang S Y et al., 2012
04CJ4-1	大渡河	河沙	LA-ICP-MS	Yang S Y et al., 2012
CJ7-4	大渡河	河沙	LA-ICP-MS	Yang S Y et al., 2012
CJ8-2	岷江	河沙	LA-ICP-MS	Yang S Y et al., 2012
CJ8-3	岷江	河沙	LA-ICP-MS	Yang S Y et al., 2012
CJ14-2	沱江	河沙	LA-ICP-MS	Yang S Y et al., 2012
CJ19-3	嘉陵江	河沙	LA-ICP-MS	Yang S Y et al., 2012
CJ20-4	乌江	河沙	LA-ICP-MS	Yang S Y et al., 2012
CJ20-5	乌江	河沙	LA-ICP-MS	Yang S Y et al., 2012
04CJ15-1	沅江	河沙	LA-ICP-MS	Yang S Y et al., 2012
04CJ15-2	沅江	河沙	LA-ICP-MS	Yang S Y et al., 2012
XJ-2	湘江	河沙	LA-ICP-MS	Yang S Y et al., 2012
04CJ17-1	汉江	河沙	LA-ICP-MS	Yang S Y et al., 2012
CJ02-1	武汉	河沙	LA-ICP-MS	Liang Z W et al., 2018
CJ02-2	武汉	河沙	LA-ICP-MS	Liang Z W et al., 2018
09TTH04	格尔木市	河沙	LA-ICP-MS	Liang Z W et al., 2018
09TTH02	曲麻莱县	河沙	LA-ICP-MS	Liang Z W et al., 2018
YNJSJ	丽江	河沙	LA-ICP-MS	Liang Z W et al., 2018
CJ04	重庆	河沙	LA-ICP-MS	Liang Z W et al., 2018
CJ02	武汉	河沙	LA-ICP-MS	Liang Z W et al., 2018
CJ07	上海	河沙	LA-ICP-MS	Liang Z W et al., 2018
HJ02	汉江	河沙	LA-ICP-MS	Liang Z W et al., 2018
JLJ02	嘉陵江	河沙	LA-ICP-MS	Liang Z W et al., 2018
HJ01	汉江	河沙	LA-ICP-MS	Liang Z W et al., 2018
TTH	沱沱河	河沙	LA-ICP-MS	He M Y et al., 2013

续表1

长江流域河沙(n=59)				
样品号	采样位置	岩性	分析方法	参考文献
SG	石鼓	河沙	LA-ICP-MS	He M Y et al., 2013
PZH1	攀枝花	河沙	LA-ICP-MS	He M Y et al., 2013
PZH2	攀枝花	河沙	LA-ICP-MS	He M Y et al., 2013
YB	宜宾	河沙	LA-ICP-MS	He M Y et al., 2013
CQ	重庆	河沙	LA-ICP-MS	He M Y et al., 2013
FL	涪陵	河沙	LA-ICP-MS	He M Y et al., 2013
YC	宜昌	河沙	LA-ICP-MS	He M Y et al., 2013
YY1	岳阳	河沙	LA-ICP-MS	He M Y et al., 2013
YY2	岳阳	河沙	LA-ICP-MS	He M Y et al., 2013
WH	武汉	河沙	LA-ICP-MS	He M Y et al., 2013
HK	湖口	河沙	LA-ICP-MS	He M Y et al., 2013
DT	大同	河沙	LA-ICP-MS	He M Y et al., 2013
NJ	南京	河沙	LA-ICP-MS	He M Y et al., 2013
CX	长兴岛	河沙	LA-ICP-MS	He M Y et al., 2013
YLJ	雅砻江	河沙	LA-ICP-MS	He M Y et al., 2013
DDH	大渡河	河沙	LA-ICP-MS	He M Y et al., 2013
MJ1	岷江	河沙	LA-ICP-MS	He M Y et al., 2013
MJ2	岷江	河沙	LA-ICP-MS	He M Y et al., 2013
JLJ	嘉陵江	河沙	LA-ICP-MS	He M Y et al., 2013
WJ	乌江	河沙	LA-ICP-MS	He M Y et al., 2013
HJ	汉江	河沙	LA-ICP-MS	He M Y et al., 2013
XJ	湘江	河沙	LA-ICP-MS	He M Y et al., 2013
GJ	赣江	河沙	LA-ICP-MS	He M Y et al., 2013
YZ1	南京	河沙	LA-ICP-MS	Iizuka et al., 2010
沉积盖层(n=42)				
样品号	采样位置	岩性	分析方法	文献
YC-1	扬子地块	变质砂岩	LA-ICP-MS	Wang L J et al., 2013
YC-2	扬子地块	冰碛岩	LA-ICP-MS	Wang L J et al., 2013
YC-6	扬子地块	变质砂岩	LA-ICP-MS	Wang L J et al., 2013
YX-1	扬子地块	片岩	LA-ICP-MS	Wang L J et al., 2013
YX-21-2	扬子地块	石英片岩	LA-ICP-MS	Wang L J et al., 2013
YX-8-1	扬子地块	砂岩	LA-ICP-MS	Wang L J et al., 2013
YX-8-2	扬子地块	砂岩	LA-ICP-MS	Wang L J et al., 2013
YX-11	扬子地块	砂岩	LA-ICP-MS	Wang L J et al., 2013
XLS01	扬子地块	变沉积岩	LA-ICP-MS	Cui X Z et al., 2022
TA07	扬子地块	变沉积岩	LA-ICP-MS	Cui X Z et al., 2022
BJQ08	扬子地块	变沉积岩	LA-ICP-MS	Cui X Z et al., 2022
99KD52	扬子地块	变沉积岩	SHRIMP-II ion microprobe	Li Z X et al., 2002
SZY8	华夏地块	矽卡岩	LA-ICP-MS	Jiang W C et al.,2019
07SC13	华夏地块	砂岩	LA-ICP-MS	Jiang W C et al.,2019
07SC31	华夏地块	砂岩	LA-ICP-MS	Jiang W C et al.,2019
07SC36	华夏地块	砂岩	LA-ICP-MS	Jiang W C et al.,2019
07SC38-1	华夏地块	砂岩	LA-ICP-MS	Jiang W C et al.,2019
07SC38-2	华夏地块	砂岩	LA-ICP-MS	Jiang W C et al.,2019

续表1

沉积盖层（n=42）				
样品号	采样位置	岩性	分析方法	文献
15LXQ-2	华夏地块	砂岩	LA-ICP-MS	Song F et al., 2020
15NH-10	华夏地块	砂岩	LA-ICP-MS	Song F et al., 2020
15NH-22	华夏地块	砂岩	LA-ICP-MS	Song F et al., 2020
LJX-19	扬子地块	砂岩	LA-ICP-MS	Song F et al., 2020
XM15-08	扬子地块	砂岩	LA-ICP-MS	Zhong N et al., 2017
XM15-01	扬子地块	湖相沉积物	LA-ICP-MS	Zhong N et al., 2017
GB133	松潘-甘孜地块	砂岩	LA-ICP-MS	Wang B Q et al., 2013
GB101	松潘-甘孜地块	砂岩	LA-ICP-MS	Wang B Q et al., 2013
GB77	松潘-甘孜地块	砂岩	LA-ICP-MS	Wang B Q et al., 2013
GB185	松潘-甘孜地块	砂岩	LA-ICP-MS	Wang B Q et al., 2013
BQ156	松潘-甘孜地块	砂岩	LA-ICP-MS	Wang B Q et al., 2013
BQ23	松潘-甘孜地块	砂岩	LA-ICP-MS	Wang B Q et al., 2013
BQ114	松潘-甘孜地块	砂岩	LA-ICP-MS	Wang B Q et al., 2013
SN14-1	扬子地块	变泥质岩	LA-MC-ICP-MS	Hu J et al., 2013
DL15	扬子地块	湖相沉积物	LA-ICP-MS	Wang K et al., 2018a
LX15	扬子地块	页岩	LA-ICP-MS	Zhong N et al., 2017
LX14	扬子地块	湖相沉积物	LA-ICP-MS	Zhong N et al., 2017
WC15	扬子地块	砂岩	LA-ICP-MS	Zhong N et al., 2017
DY15	扬子地块	粉尘沉积物	LA-ICP-MS	Zhong N et al., 2017
YG-2001	扬子地块	石英片岩	LA-ICP-MS	殷桂芹等，2022
YG-2002	扬子地块	石英片岩	LA-ICP-MS	殷桂芹等，2022
YG-2003	扬子地块	石英片岩	LA-ICP-MS	殷桂芹等，2022
02KD176	扬子地块	石英云母片岩	SHRIMP	Greentree and Li Z X, 2008
XZ0701	羌塘	石英岩	SHRIMP	Dong C Y et al., 2011
结晶基底（n=130）				
样品号	采样位置	岩性	分析方法	文献
15KL01-2	扬子地块	片麻岩	LA-ICP-MS	Liu B et al., 2019
15KL11-1	扬子地块	片麻岩	LA-ICP-MS	Liu B et al., 2019
15KL13-4	扬子地块	片麻岩	LA-ICP-MS	Liu B et al., 2019
D0002-1	扬子地块	黑云母-透闪石片岩	LA-ICP-MS	Wei Y X et al., 2019
D0002-2	扬子地块	英云闪长质片麻岩类	LA-ICP-MS	Wei Y X et al., 2019
D0002-3	扬子地块	奥长花岗片麻岩	LA-ICP-MS	Wei Y X et al., 2019
D0002-4	扬子地块	片麻状花岗岩	LA-ICP-MS	Wei Y X et al., 2019
D0002-5	扬子地块	钾长花岗岩脉	LA-ICP-MS	Wei Y X et al., 2019
11YC01	扬子地块	镁铁质麻粒岩	LA-ICP-MS	Han P Y et al., 2017
11YC2	扬子地块	石榴石-矽线石片麻岩	LA-ICP-MS	Han P Y et al., 2017
11YC01-6	扬子地块	镁铁质麻粒岩	LA-ICP-MS	Yin Y C et al., 2013
11YC2-2	扬子地块	片麻岩	LA-ICP-MS	Yin Y C et al., 2013
11YC2-8	扬子地块	片麻岩	LA-ICP-MS	Yin Y C et al., 2013
11YC2-11	扬子地块	片麻岩	LA-ICP-MS	Yin Y C et al., 2013
11YC05-7	扬子地块	大理岩	LA-ICP-MS	Yin Y C et al., 2013
11YC06-1	扬子地块	花岗岩	LA-ICP-MS	Yin Y C et al., 2013
LS-16	华夏地块	片麻状花岗岩	SHRIMP	Wang Z J et al., 2015

续表1

结晶基底(*n*=130)				
样品号	采样位置	岩性	分析方法	文献
ZJ06-15	华夏地块	片麻岩	LA-ICP-MS	Yu J H et al., 2009
ZJ06-21	华夏地块	花岗岩	LA-ICP-MS	Yu J H et al., 2009
ZJ06-23	华夏地块	片麻岩	LA-ICP-MS	Yu J H et al., 2009
ZJ06-31	华夏地块	花岗岩	LA-ICP-MS	Yu J H et al., 2009
ZJ06-35	华夏地块	花岗岩	LA-ICP-MS	Yu J H et al., 2009
ZJ06-39	华夏地块	花岗岩	LA-ICP-MS	Yu J H et al., 2009
LS-61-1	华夏地块	花岗岩	LA-ICP-MS	Liu Q et al., 2014
LS-11	华夏地块	花岗岩	LA-ICP-MS	Liu Q et al., 2014
LS-12-2	华夏地块	花岗岩	LA-ICP-MS	Liu Q et al., 2014
LS-21	华夏地块	花岗岩	LA-ICP-MS	Liu Q et al., 2014
LS-23	华夏地块	花岗岩	LA-ICP-MS	Liu Q et al., 2014
LS-24-2	华夏地块	花岗岩	LA-ICP-MS	Liu Q et al., 2014
LS-28	华夏地块	花岗岩	LA-ICP-MS	Liu Q et al., 2014
LS-33-4	华夏地块	花岗岩	LA-ICP-MS	Liu Q et al., 2014
WY01	华夏地块	花岗岩	LA-SS-ICP-MS	Zhao L et al., 2014
WY02	华夏地块	花岗岩	LA-SS-ICP-MS	Zhao L et al., 2014
WY06	华夏地块	花岗岩	LA-SS-ICP-MS	Zhao L et al., 2014
WY07	华夏地块	花岗岩	LA-SS-ICP-MS	Zhao L et al., 2014
F1	华夏地块	辉绿岩脉	LA-ICP-MS	Peng S B et al., 2012
F2	华夏地块	辉长岩	LA-ICP-MS	Peng S B et al., 2012
09M042	华夏地块	变辉长岩	LA-ICP-MS	Peng S B et al., 2012
09G078	华夏地块	变伟晶辉长岩	LA-ICP-MS	Peng S B et al., 2012
Gra1	华夏地块	花岗岩	LA-ICP-MS	Peng S B et al., 2012
Gra6	华夏地块	花岗岩	LA-ICP-MS	Peng S B et al., 2012
Gra9	华夏地块	花岗岩	LA-ICP-MS	Peng S B et al., 2012
11HB06-3	华夏地块	凝灰岩	LA-MC-ICP-MS	Li H et al., 2013
09WG66A	华夏地块	角闪岩	SHRIMP	Wang Y J et al., 2013
09WG53A	华夏地块	变辉绿岩	SIMS	Wang Y J et al., 2013
13QL27	扬子地块	奥长花岗片麻岩	SHRIMP II	Zhang S B et al., 2020
13QL30	扬子地块	变镁铁质岩	SHRIMP II	Zhang S B et al., 2020
13QL31	扬子地块	变中性岩	SHRIMP-RG ion microprobe	Zhang S B et al., 2020
15QL33	扬子地块	变镁铁质岩	SHRIMP-RG ion microprobe	Zhang S B et al., 2020
13JM05	扬子地块	花岗岩	SHRIMP II	Zhang S B et al., 2020
15QL34	扬子地块	变镁铁质岩	LA-ICP-MS	Zhang S B et al., 2020
D221-1	扬子地块	花岗片麻岩	LA-ICP-MS	Zhao T et al., 2021
D14-1	扬子地块	花岗片麻岩	LA-ICP-MS	Zhao T et al., 2021
D118-1	扬子地块	花岗片麻岩	LA-ICP-MS	Zhao T et al., 2021
CK01-01	扬子地块	二长花岗岩	SHRIMP	Cui X Z et al., 2020
CK02-07	扬子地块	二长花岗岩	SHRIMP	Cui X Z et al., 2020
CK03-12	扬子地块	二长花岗岩	SHRIMP	Cui X Z et al., 2020
MJC03-16	扬子地块	花岗片麻岩	SHRIMP	Cui X Z et al., 2020
YDZ-01	扬子地块	TTG 片麻岩	LA-ICP-MS	Hui B et al., 2017
YDZ-18	扬子地块	斜长角闪片麻岩	LA-ICP-MS	Hui B et al., 2017
YDZ-25	扬子地块	黑云斜长片麻岩	LA-ICP-MS	Hui B et al., 2017
YDZ-13	扬子地块	角闪岩	LA-ICP-MS	Hui B et al., 2017

续表1

结晶基底（n=130）				
样品号	采样位置	岩性	分析方法	文献
D51-7-2	扬子地块	花岗岩	LA-ICP-MS	Xu D L et al., 2018
13BZ01-2	扬子地块	流纹岩	LA-ICP-MS	Han Q S et al., 2019
14WD-01	扬子地块	钾长花岗岩	LA-ICP-MS	Han Q S et al., 2019
13MY-05	扬子地块	片麻状花岗闪长岩	LA-ICP-MS	Han Q S et al., 2019
14MY-2A	扬子地块	片麻状花岗闪长岩	LA-ICP-MS	Han Q S et al., 2019
W1	扬子地块	二长花岗岩	LA-ICP-MS	Han Q S et al., 2019
W2	扬子地块	正长岩	LA-ICP-MS	Han Q S et al., 2019
15SJ-01	扬子地块	片麻状二长花岗岩	LA-ICP-MS	Han Q S et al., 2019
14SJ-04	扬子地块	片麻状二长花岗岩	LA-ICP-MS	Han Q S et al., 2019
PS3	扬子地块	云斜煌斑岩	SHRIMP	Jiang S H et al., 2009
YDP4	扬子地块	辉长岩	SHRIMP	Jiang S H et al., 2009
YDP11	扬子地块	辉长岩	SHRIMP	Jiang S H et al., 2009
YDP6	扬子地块	石英闪长岩	SHRIMP	Jiang S H et al., 2009
YDP7	扬子地块	花岗闪长岩	SHRIMP	Jiang S H et al., 2009
YDP8	扬子地块	花岗岩	SHRIMP	Jiang S H et al., 2009
YDP10	扬子地块	花岗岩	SHRIMP	Jiang S H et al., 2009
H1	秦岭	花岗岩	LA-ICP-MS	Wang T et al., 2009
QY03	秦岭	花岗岩	LA-ICP-MS	Dong Y P et al., 2011
QY04	秦岭	花岗岩	LA-ICP-MS	Dong Y P et al., 2011
QY06	秦岭	花岗岩	LA-ICP-MS	Dong Y P et al., 2011
97HN36	华夏地块	花岗闪长岩	SHRIMP-II ion microprobe	Li Z X et al., 2002
97HN93	华夏地块	花岗闪长岩	SHRIMP-II ion microprobe	Li Z X et al., 2002
99KD33	扬子地块	花岗片麻岩	SHRIMP-II ion microprobe	Li Z X et al., 2002
98KD75	扬子地块	镁铁质岩脉	SHRIMP-II ion microprobe	Li Z X et al., 2002
maoergai	松潘-甘孜地块	花岗岩	SHRIMP II	胡建民等，2005
xinduqiao	松潘-甘孜地块	花岗岩	SHRIMP II	胡建民等，2005
huanglian	松潘-甘孜地块	花岗岩	SHRIMP II	胡建民等，2005
yajiang	松潘-甘孜地块	花岗岩	SHRIMP II	胡建民等，2005
siguniang	松潘-甘孜地块	花岗岩	SHRIMP II	胡建民等，2005
KH112	扬子地块	花岗片麻岩	LA-ICP-MS	Guo J L et al., 2014
12ZX03	扬子地块	花岗岩	LA-ICP-MS	Zhou G Y et al., 2017
12ZX07	扬子地块	花岗岩	LA-ICP-MS	Zhou G Y et al., 2017
LSH-1	扬子地块	片麻状花岗岩	LA-ICP-MS	Wang Z J et al., 2015
zx12-1	扬子地块	二长花岗岩	LA-ICP-MS	Wang K and Dong S W, 2019
zx13-1	扬子地块	二长花岗岩	LA-ICP-MS	Wang K and Dong S W, 2019
zx14-1	扬子地块	钾长花岗岩	LA-ICP-MS	Wang K and Dong S W, 2019
zx15-1	扬子地块	钾长花岗岩	LA-ICP-MS	Wang K and Dong S W, 2019
YDZ3-1	扬子地块	黑云母花岗岩	LA-ICP-MS	张欣等，2010
YDZ6-1	扬子地块	黑云母花岗岩	LA-ICP-MS	张欣等，2010
XX09-1	扬子地块	片麻岩	LA-MC-ICP-MS	Hu J et al., 2013
XX43-2	扬子地块	片麻岩	LA-MC-ICP-MS	Hu J et al., 2013
XP08-4	扬子地块	片麻岩	LA-MC-ICP-MS	Hu J et al., 2013
XP16-4	扬子地块	片麻岩	LA-MC-ICP-MS	Hu J et al., 2013
SN07-7	扬子地块	片麻岩	LA-MC-ICP-MS	Hu J et al., 2013
07QL14	扬子地块	片麻岩	LA-ICP-MS	Wu Y B et al., 2012

续表1

结晶基底(*n*=130)				
样品号	采样位置	岩性	分析方法	文献
DL-500	扬子地块	花岗片麻岩	LA-ICP-MS	Chen Z H and Xing G F, 2016
DL-640	扬子地块	花岗片麻岩	LA-ICP-MS	Chen Z H and Xing G F, 2016
KH119	扬子地块	A型花岗片麻岩	LA-ICP-MS	Chen K et al., 2013
KH131	扬子地块	A型花岗片麻岩	LA-ICP-MS	Chen K et al., 2013
KH132	扬子地块	花岗片麻岩	LA-ICP-MS	Chen K et al., 2013
KH163	扬子地块	花岗片麻岩	LA-ICP-MS	Chen K et al., 2013
KH174	扬子地块	A型花岗片麻岩	LA-ICP-MS	Chen K et al., 2013
KH175	扬子地块	斜长角闪片麻岩	LA-ICP-MS	Chen K et al., 2013
KH183	扬子地块	斜长角闪片麻岩	LA-ICP-MS	Chen K et al., 2013
KH184	扬子地块	花岗片麻岩	LA-ICP-MS	Chen K et al., 2013
LH12	扬子地块	片麻状花岗岩	LA-ICP-MS	Cui X Z et al., 2021
ZX04-1	扬子地块	钾质花岗岩	LA-ICP-MS	Wang K et al., 2018a
ZX06-1	扬子地块	黑云二长花岗岩	LA-ICP-MS	Wang K et al., 2018a
ZX06-2	扬子地块	黑云二长花岗岩	LA-ICP-MS	Wang K et al., 2018a
ZX08-1	扬子地块	花岗岩	LA-ICP-MS	Wang K et al., 2018a
ZX09-1	扬子地块	花岗岩	LA-ICP-MS	Wang K et al., 2018a
SN16-2	扬子地块	片麻岩	LA-MC-ICP-MS	Wu Y B et al., 2014
XX41-1	扬子地块	片麻岩	LA-MC-ICP-MS	Wu Y B et al., 2014

来自长江流域现代河流沉积物中的碎屑锆石颗粒，记录了约2900~2480 Ma、2100~1850 Ma、1200~750 Ma、560~410 Ma和250~180 Ma的五次主要岩浆事件(图3)。对不同年龄段的碎屑锆石以及对应基底岩浆锆石数据使用Dröllner et al.(2022)的方法进行α-dose计算，结果见表2。

表2　长江干流现代河流沉积物、沉积盖层碎屑锆石和结晶基底岩浆锆石不同年龄段的α-dose计算结果

Table 2　The α-dose calculation results of different age stages for detrital zircons from Yangtze River mainstream modern river sediments, related sedimentary rocks, and magmatic zircons of crystalline basement

	年龄峰值	α-dose值分布范围	α-dose平均值	α-dose值中位数
现代河流沉积物	2900~2480 Ma	3.1×10^{16}~5.4×10^{13}	2.9×10^{15}	1.8×10^{15}
	2100~1850 Ma	1.9×10^{16}~7.5×10^{12}	2.2×10^{15}	1.9×10^{15}
	1200~750 Ma	1.4×10^{16}~1.2×10^{13}	9.4×10^{14}	5.9×10^{14}
	560~410 Ma	5.0×10^{16}~8.1×10^{13}	7.1×10^{14}	5.1×10^{14}
	250~180 Ma	4.9×10^{15}~4.2×10^{12}	4.6×10^{14}	3.5×10^{14}
沉积盖层	2900~2480 Ma	7.1×10^{15}~1.0×10^{14}	2.6×10^{15}	2.3×10^{15}
	2100~1850 Ma	1.2×10^{16}~1.1×10^{14}	2.4×10^{15}	1.8×10^{15}
	1200~750 Ma	3.2×10^{15}~5.6×10^{13}	1.1×10^{15}	8.8×10^{14}
	560~410 Ma	4.8×10^{15}~9.8×10^{13}	7.3×10^{14}	5.8×10^{14}
	250~180 Ma	4.2×10^{15}~1.8×10^{13}	5.1×10^{14}	4.0×10^{14}
结晶基底	2900~2480 Ma	7.1×10^{16}~1.8×10^{14}	3.3×10^{15}	2.5×10^{15}
	2100~1850 Ma	3.8×10^{16}~4.9×10^{13}	2.9×10^{15}	1.8×10^{15}
	1200~750 Ma	8.3×10^{15}~7.2×10^{13}	1.2×10^{15}	7.9×10^{14}
	560~410 Ma	1.5×10^{16}~1.0×10^{14}	1.7×10^{15}	9.7×10^{14}
	250~180 Ma	3.4×10^{15}~1.6×10^{13}	5.8×10^{14}	3.9×10^{14}

对于同一锆石年龄组的结果来说，潜在源区基底岩石的锆石、沉积岩地层中碎屑锆石和长江干流现代沉积物中碎屑锆石计算得到的α-dose均值逐步减小（图4），归一化的α-dose值显示三类锆石的最低值变化不大，而最高值明显下降（图5）。如果这些碎屑锆石的最初来源是流域内的基岩，那么这种现象说明基岩锆石在进入沉积系统后可能经历了沉积再循环过程，导致具有相对高U、Th含量（具有更高的放射性损伤）的颗粒分解或磨蚀。不同年龄组锆石的对比可以发现，年龄段较年轻的锆石源归一化α-dose值差异较小，例如250~180 Ma和560~410 Ma年龄段的锆石源归一化α-dose值分布范围、均值以及中位数差异很小；而年龄段较老的锆石在不同来源的数据集中源归一化α-dose值变化更为明显。这可能是因为较年轻的碎屑锆石由年轻的岩浆岩风化剥蚀而来，它们经历多次再循环过程的次数相对于古老的锆石偏少，而古老结晶基底风化剥蚀的锆石经历（多次）沉积再循环的可能性更高。

此外，前人对扬子地块西部和东部结晶基底的对比研究发现，扬子地块西部晚太古代至古元古代的岩浆变质事件的时代和性质与东部陆核区有显著差别（Wang W et al., 2016; Zhou G Y et al., 2018）。碎屑锆石U-Pb年龄的统计对比和结晶基底的研究进一步揭示了扬子地块西部有强烈的2.40~2.05 Ga的岩浆活动（Wu Y B et al., 2012; Cui X Z et al., 2019, 2020）。但是，在扬子地块东部（长江中下游地区）的结晶基底中记录较少，且碎屑锆石的记录也较少，仅在支流嘉陵江上游后河地区和干流的宜昌地区有报道（Wu Y B et al., 2012; Guo J L et al., 2015; Han Q S et al., 2018）。因此，早古元古代的碎屑锆石可以作为识别长江上游物质贡献的一个重要依据。统计结果显示长江上游地区结晶基底中2.40~2.05 Ga的岩浆锆石α-dose值分布范围为1.9×10^{14}~2.5×10^{16}，均值为3.4×10^{15}，中位数为2.5×10^{15}；长江流域沉积物中2.40~2.05 Ga的岩浆锆石α-dose

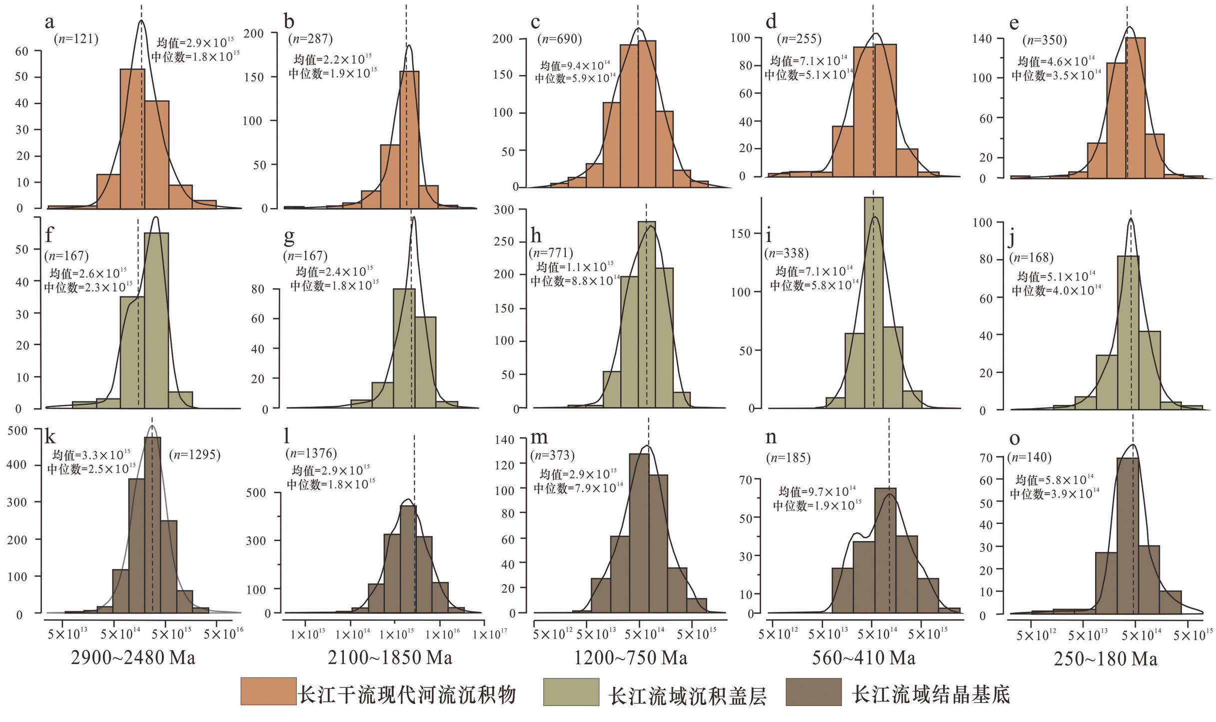

图4 长江干流现代河流沉积物、流域内沉积盖层的碎屑锆石和流域内结晶基底不同年龄段锆石U-Pb年代学数据计算的α-dose值分布、均值以及中位数

Fig. 4 The α-dose distribution, mean, and median values calculated from U-Pb geochronological data of detrital zircons from modern river sediments of the Yangtze River mainstream, and related sedimentary rocks, and magmatic zircons from crystalline basement

图中纵向虚线代表样品中位数分布情况

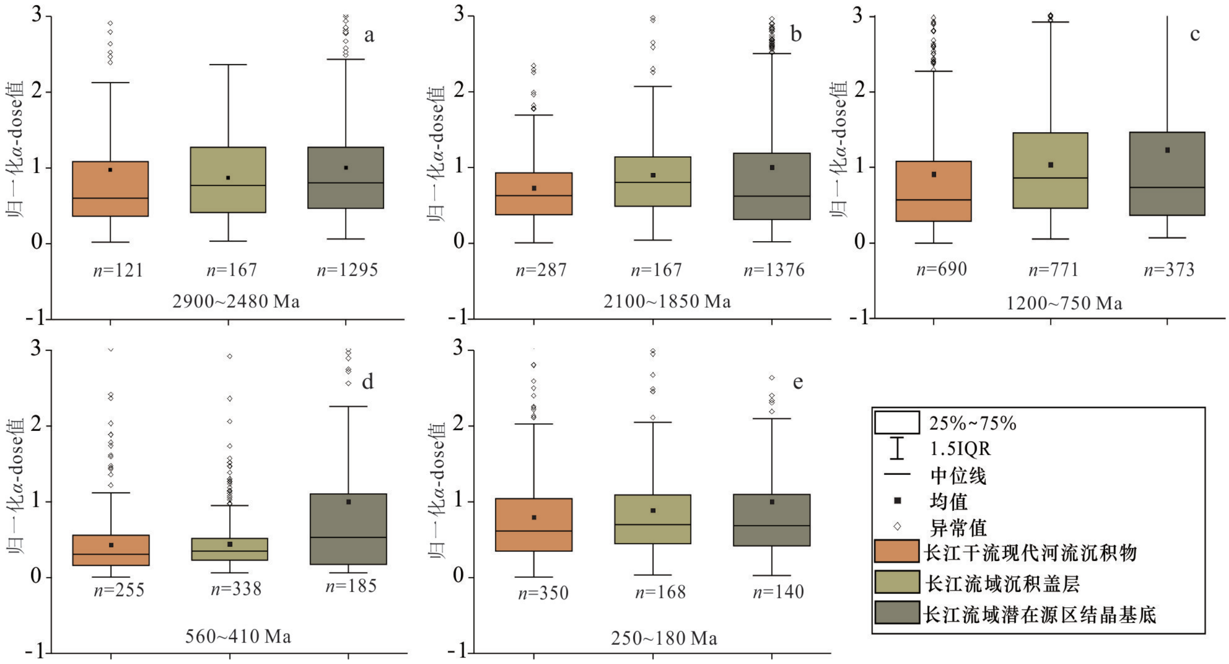

图5　长江干流现代河流沉积物和流域内沉积盖层碎屑锆石，以及结晶基底的岩浆锆石中不同年龄段的颗粒源归一化α-dose值分布、均值和中位数

Fig. 5　The source normalized α-dose distribution, mean, and median values of detrital zircons in modern river sediments, related sedimentary rocks, and magmatic zircons from crystalline basement in the Yangtze River mainstream drainage basin

值分布范围为3.1×10^{14}~2.8×10^{16}，均值为3.2×10^{15}，中位数为2.5×10^{15}；长江上游干流中2.40~2.05 Ga的碎屑锆石α-dose值分布范围为7.5×10^{12}~8.1×10^{16}，均值为1.8×10^{15}，中位数为1.5×10^{15}；长江中下游干流中2.40~2.05 Ga的碎屑锆石α-dose值分布范围为3.9×10^{14}~9.5×10^{15}，均值为2.3×10^{15}，中位数为1.6×10^{15}。

对比长江上游内措科地区结晶基底的2.40~2.05 Ga锆石和沉积盖层中这一年龄段的碎屑锆石α-dose和源归一化α-dose值，二者的差异不大，最高值略有降低(图6)。但是在长江上游干流中，该河段的碎屑锆石同一年龄组的锆石α-dose和源归一化α-dose值的均值和最高值都有明显降低。2.40~2.05 Ga的碎屑锆石主要出现在中元古代的沉积盖层中，是这一地区目前发现最古老的沉积记录，对应中元古代的构造拉伸阶段的沉积盆地，因此，早古元古代的岩浆结晶基底经历风化剥蚀后可能没有经历多次的沉积再循环作用。相较而言，现代沉积物中该年龄段碎屑锆石源归一化α-dose值的显著降低说明了这些锆石不太可能是由结晶基底或者古元古代地层直接风化剥蚀的产物。此外，长江上游距离措科地区和中元古代沉积岩出露地区距离较近，也不太可能存在由于距离搬运导致的高放射性损伤锆石组分丢失。因此，我们统计的数据结果显示长江上游的早古元古代碎屑锆石可能经历了多次的沉积再循环作用。长江中下游地区2.40~2.05 Ga的碎屑锆石的源归一化α-dose值相对于中上游有明显升高，这种现象说明它们不太可能全部来源于现代长江上游，而是有其他的物源区提供高α-dose值的碎屑锆石。宜昌地区的崆岭杂岩可能是提供这些锆石的一个重要物源区，这说明长江下游水系的碎屑锆石不是全部直接来源于上游高海拔地区的风化剥蚀。虽然整个长江流域的碎屑锆石U-Pb年龄谱具有高度的相似性，但是这种相似性可能是受到沉积再循环作用的影响：在不同时期的沉积盆地内，各种来源的锆石充分混合，经历多次的沉积再循环后进入长江流域现代水系沉积物。

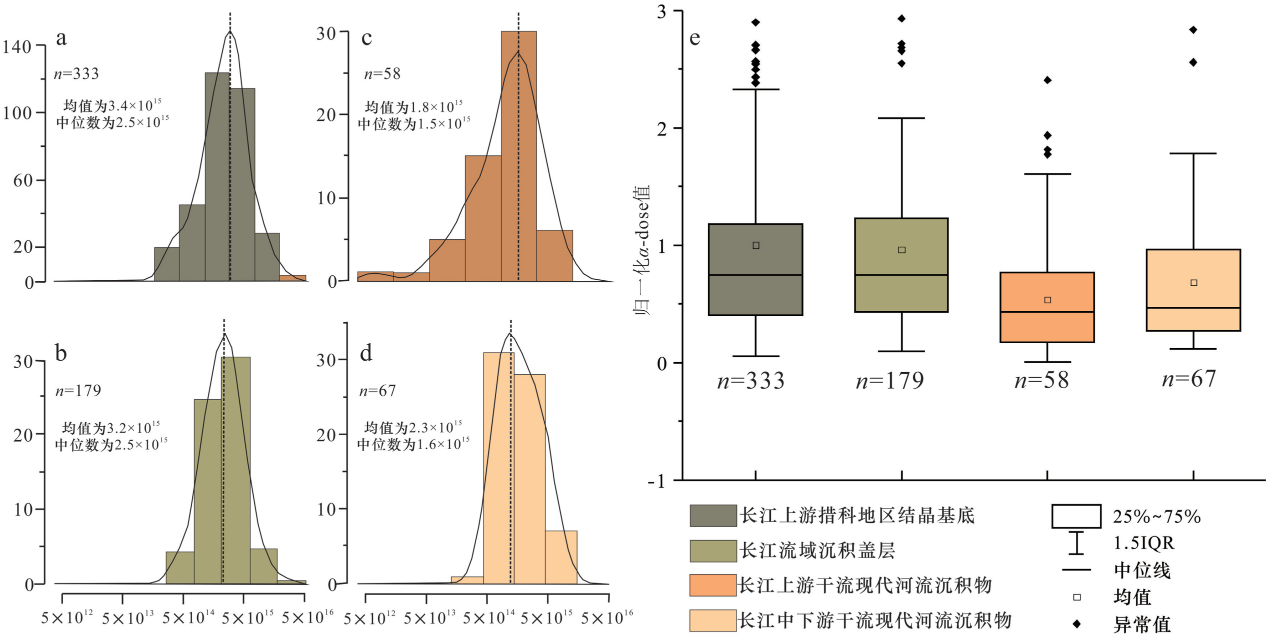

图6 长江干流现代河流沉积物、流域内沉积盖层的碎屑锆石和长江流域上游措科地区结晶基底2.40~2.05 Ga 锆石α-dose值分布和归一化α-dose值对比

Fig. 6 The source normalized α-dose distribution, mean, and median values of detrital zircons with U-Pb age between 2.40 and 2.05 Ga in modern river sediments, related sedimentary rocks, and magmatic zircons from crystalline basement in the Yangtze River drainage basin

3 结语

沉积再循环作用普遍存在，是严重影响碎屑锆石数据解释的重要因素。近年来，越来越多的研究通过不同手段揭示了地质历史时期和现代沉积物中存在大比例的、经历多次沉积再循环的锆石。通过检查碎屑矿物的沉积自生边以及对沉积自生矿物进行精细的年代学分析，可以确定沉积岩风化剥蚀的物质来源。沉积岩的矿物成熟度和地球化学指标不同程度地受到水动力分选、风化搬运磨蚀和源区化学风化强度的影响，联合多个地球化学指标可能是证明再循环碎屑锆石存在的有效方法。锆石的低温热年代学结合U-Pb年代学研究可以重建锆石结晶之后的热历史，为锆石来源提供更多的制约，但大部分情况下可能不能准确辨别沉积再循环锆石和变质结晶基底来源的锆石。联合其他碎屑矿物和锆石记录的研究手段可以提供更丰富的物源信息，但是鉴于不同矿物在矿物成因、不同岩石中的丰度和地表过程中稳定性的差异，对沉积再循环锆石的鉴别需要结合区域沉积历史和构造演化历史进行充分地论证。通过计算碎屑锆石的放射性损伤强度（α-dose值）与物源区的基岩数据对比，揭示沉积再循环过程中的蜕晶化锆石的选择性丢失，可以评估碎屑锆石经历沉积再循环作用的强度，不过该方法的前提是能够明确锆石结晶的寄主岩石信息。总之，虽然很多研究在不同地区的沉积岩中识别出了沉积再循环碎屑锆石，但是目前还没有十分通用有效的判别方法。

本文系统收集了长江干流和支流的碎屑锆石、流域内基岩的岩浆锆石和沉积盖层的碎屑锆石U-Pb年代学数据，通过计算α-dose值，并进行比对，论证了长江流域内的碎屑锆石中可能存在大量的来自沉积盖层的再循环锆石，这些锆石的存在使得利用碎屑锆石U-Pb分布的物源分析存在很大的不确定性。

参考文献：

胡健民,孟庆任,石玉若,渠洪杰.2005.松潘-甘孜地块内花岗岩锆石SHRIMP U-Pb定年及其构造意义[J].岩石学报,

21(3):867-880.
刘伯根,郑光财,陈时淼,唐红峰.1995.浙西松木坞群的解体——同位素定年的证据[J].地质论评,41(5):457-462.
舒良树,施央申,郭令智.1995.江南中段板块-地体构造与碰撞造山运动学[M].南京:南京大学出版社.
舒良树,周国庆.1988.赣北元古代地体拚贴带中高压变质矿物的发现及其构造意义[J].南京大学学报(自然科学版),24(3):421-429.
王孝磊.2006.江南造山带西段中-新元古代构造—岩浆演化[D].南京大学博士学位论文.
魏君奇,王建雄.2012.崆岭杂岩中斜长角闪岩包体的锆石年龄和Hf同位素组成[J].高校地质学报,18(4):589-600.
吴荣新,郑永飞,吴元保.2005.皖南蛇绿岩套辉长岩锆石U-Pb定年以及元素和氧同位素研究[J].地球学报,26(S1):70-73.
吴元保,郑永飞.2004.锆石成因矿物学研究及其对U-Pb年龄解释的制约[J].科学通报,49(16):1589-1604.
殷桂芹,陈友良,张宝玲,顾孟娟,王 勤,姚 建,尹 观.2022.四川米易垭口地区前震旦纪五马箐组与其侵入岩体的锆石U-Pb年代学、Lu-Hf同位素特征及其地质意义[J].岩石学报,38(4):1126-1148.
曾 雯,周汉文,钟增球,曾昭光,李惠民.2005.黔东南新元古代岩浆岩单颗粒锆石U-Pb年龄及其构造意义[J].地球化学,34(6):548-556.
张 欣,徐学义,宋公社,王洪亮,陈隽璐,李 婷.2010.西秦岭略阳地区鱼洞子杂岩变形花岗岩锆石LA-ICP-MS U-Pb测年及地质意义[J].地质通报,29(4):510-517.
钟玉芳,马昌前,佘振兵,林广春,续海金,王人镜,杨坤光,刘强.2005.江西九岭花岗岩类复式岩基锆石SHRIMP U-Pb年代学[J].地球科学,30(6):685-691.
周国庆,舒良树,吴洪亮.1989.与赣东北元古代蛇绿岩有关的高温、高压变质岩和重变质作用机制的讨论[J].岩石矿物学杂志,8(3):220-231+219.
Andersen T, van Niekerk H, Elburg M A. 2022. Detrital zircon in an active sedimentary recycling system: Challenging the‘source-to-sink’approach to zircon-based provenance analysis[J]. Sedimentology, 69: 2436-2462.
Anderson J B, Wallace D J, Simms A R, Rodriguez A B, Weight R W R, Taha Z P. 2016. Recycling sediments between source and sink during a eustatic cycle: Systems of late Quaternary northwestern Gulf of Mexico Basin[J]. Earth-Science Reviews, 153: 111-138.
Balan E, Neuville D R, Trocellier P, Fritsch E, Muller J P, Calas G. 2001. Metamictization and chemical durablity of detrital zircon[J]. American Mineralogist, 86: 1025-1033.
Barham M, Kirkland C L, Hovikoski J, Alsen P, Hollis J, Tyrell S. 2021. Reduce or recycle? Revealing source to sink links through integrated zircon-feldspar provenance fingerprinting[J]. Sedimentology, 68: 531-556.
Basu A, Schieber J, Patranabis-Deb S, Dhang P C. 2013. Recycled detrital quartz grains are sedimentary rock fragments indicating unconformities: examples from the Chhattisgarh Supergroup, Bastar Craton, India[J]. Journal of Sedimentary research, 83: 368-376.
Bernet M. 2009. A field-based estimate of the zircon fission-track closure temperature[J]. Chemical Geology, 259:181-189.
Campbell I H, Reiners P W, Allen C M, Nicolescu S, Upadhyay R. 2005. He-Pb double dating of detrital zircons from the Ganges and Indus Rivers: Implication for quantifying sediment recycling and provenance studies[J]. Earth and Planetary Science Letters, 237: 402-432.
Cawood P A, Hawkesworth C J, Dhuime B. 2012. Detrital zircon record and tectonic setting[J]. Geology, 40: 875-878.
Cawood P A, Nemchin A A, Freeman M, Sircombe K. 2003. Linking source and sedimentary basin: Detrital zircon record of sediment flux along a modern river system and implications for provenance studies[J]. Earth and Planetary Science Letters, 210:259-268.
Cawood P A, Wang W, Zhao T, Xu Y, Mulder J A, Pisarevsky S A, Zhang L, Gan C, He H, Liu H, Qi L, Wang Y, Yao J, Zhao G, Zhou M F, Zi J W. 2020. Deconstructing South China and consequences for reconstructing Nuna and Rodinia[J]. Earth Science Reviews, 204: 103169.
Chen J F, Foland K A, Xing F M, Xu X, Zhou T X. 1991. Magmatism along the southeast margin of the Yangtze block: Precambrian collision of the Yangtze and Cathysia blocks of China[J]. Geology, 19: 815-818.
Chen K, Gao S, Wu Y B, Guo J L, Hu Z C, Liu Y S, Zong K Q, Liang Z W, Geng X L. 2013. 2.6-2.7Ga crustal growth in Yangtze craton, South China[J]. Precambrian Research, 224: 472-490.
Chen Z H, Xing G F. 2016. Geochemical and zircon U-Pb-Hf-O isotopic evidence for a coherent Paleoproterozoic basement beneath the Yangtze Block, South China[J]. Precambrian Research, 279: 81-90.

Chew D, O’Sullivan G, Caracciolo L, Mark C, Tyrrell S. 2020. Sourcing the sand: Accessory mineral fertility, analytical and other biases in detrital U-Pb provenance analysis[J]. Earth-Science Reviews, 202: 103093.

Chmura G L, Smirnov A, Campbell I D. 1999. Pollen transport through distributaries and depositional patterns in coastal waters[J]. Palaeogeography, Palaeoclimatology, Palaeoecology, 149: 257-270.

Cui X Z, Ren G M, Pang W H, Chen F L, Sun Z M, Ren F, Ning K B, Deng Q. 2022. Detrital zircon provenance of metasedimentary rocks in the Proterozoic Caiziyuan-Tongan accretionary complex: Constraints on crustal and tectonic evolution of the Yangtze Block, South China[J]. Geological Journal, 57: 2094-2109.

Cui X Z, Wang J, Ren G M, Deng Q, Sun Z M, Ren F, Chen F L. 2020. Paleoproterozoic tectonic evolution of the Yangtze Block: New evidence from ca. 2.36 to 2.22 Ga magmatism and 1.96 Ga metamorphism in the Cuoke complex, SW China[J]. Precambrian Research, 337: 105525.

Cui X Z, Wang J, Sun Z M, Wang W, Deng Q, Ren G M, Liao S Y, Huang M D, Chen F L, Ren F. 2019. Early Paleoproterozoic（ca. 2.36 Ga）post-collisional granitoids in Yunnan, SW China: Implications for linkage between Yangtze and Laurentia in the Columbia supercontinent[J]. Journal of Asian Earth Sciences, 169: 308-322.

Cui X Z, Wang J, Wang X C, Wilde S A, Ren G M, Li S, Deng Q, Ren F, Liu J. 2021. Early crustal evolution of the Yangtze Block: Constraints from zircon U-Pb-Hf isotope systematics of 3.1-1.9 Ga granitoids in the Cuoke Complex, SW China[J]. Precambrian Research, 357: 106155.

Dhuime B, Hawkesworth C J, Cawood P A, Storey C D. 2012. A Change in the Geodynamics of Continental Growth 3 Billion Years Ago[J]. Science, 335: 1334-1336.

Dhuime B, Hawkesworth C J, Delavault H, Cawood P A. 2017. Continental growth seen through the sedimentary record[J]. Sedimentary Geology, 357: 16-32.

Dickinson W R, Gehrels G E. 2008. U-Pb Ages of detrital zircons in relation to paleogeography: Triassic paleodrainage networks and sediment dispersal across Southwest Laurentia[J]. Journal of Sedimentary Research, 78: 745-764.

Dickinson W R, Gehrels G E. 2009. Use of U-Pb ages of detrital zircons to infer maximum depositional ages of strata: A test against a Colorado Plateau Mesozoic database[J]. Earth and Planetary Science Letters, 288: 115-125.

Dickinson W R, Gehrels G E. 2010. Insights into North American Paleogeography and Paleotectonics from U-Pb ages of detrital zircons in Mesozoic strata of the Colorado Plateau, USA[J]. International Journal of Earth Sciences, 99: 1247-1265.

Dickinson W R. 2008. Impact of differential zircon fertility of granitoid basement rocks in North America on age populations of detrital zircons and implications for granite petrogenesis[J]. Earth and Planetary Science Letters, 275: 80-92.

Dong C Y, Li C L, Wan Y S, Wang W, Wu Y W, Xie H Q, Liu D Y. 2011. Detrital zircon age model of Ordovician Wenquan quartzite south of Lungmuco-Shuanghu Suture in the Qiangtang area, Tibet: Constraint on tectonic affinity and source regions[J]. Science China Earth Sciences, 54: 1034-1042.

Dong Y P, Genser J, Neubauer F, Zhang G W, Liu X M, Yang Z, Heberer B. 2011. U-Pb and $^{40}Ar/^{39}Ar$ geochronological constraints on the exhumation history of the North Qinling terrane, China[J]. Gondwana Research, 19（4）：881-893.

Dröllner M, Barham M, Kirkland C L, Roberts M P. 2023. Older than they look: Cryptic recycled xenotime on detrital zircon[J]. Geology, 51: 768-772.

Dröllner M, Barham M, Kirkland C L. 2022. Gaining from loss: Detrital zircon source-normalized α-dose discriminates first- versus multi-cycle grain histories[J]. Earth and Planetary Science Letters, 579: 117346.

Edwards K J, Fyfe R M, Hunt C O, Schofield J E. 2015. Moving forwards? Palynology and the human dimension[J]. Journal of Archaeological Science, Scoping the Future of Archaeological Science: Papers in Honour of Richard Klein, 56: 117-132.

Edwards K J, Pardoe H S. 2018. How palynology could have been paepalology: the naming of a discipline[J]. Palynology, 42: 4-19.

Enkelmann E, Sanchez Lohff S K, Finzel E S. 2019. Detrital zircon double-dating of forearc basin strata reveals magmatic, exhumational, and thermal history of sediment source areas[J]. Geological Society of America Bulletin, 131: 1364-1384.

Enkelmann E, Weislogel A, Ratschbacher L, Eide E, Renno

A, Wooden J. 2007. How was the Triassic Songpan-Ganzi basin filled? A provenance study[J]. Tectonics, 26(4): TC4007.

Evans J, Zalasiewicz J. 1996. U-Pb, Pb-Pb and Sm-Nd dating of authigenic monazite: implications for the diagenetic evolution of the Welsh Basin[J]. Earth and Planetary Science Letters, 144: 421-433.

Fedo C M, Sircombe K N, Rainbird R H. 2003. Detrital Zircon Analysis of the Sedimentary Record[J]. Reviews in Mineralogy and Geochemistry, 53: 277-303.

Gan C S, Qian, X, Zhang Y Z, Bai T X, Wang Y J. 2023. Provenance variation of the Cambrian-Ordovician sedimentary rocks across South China and implication for its paleogeography in East Gondwana[J]. Lithos, 454-455: 107242.

Gao J, Klemd R, Long L L, Xiong X M, Qian Q. 2009. Adakitic signature formed by fractional crystallization: An interpretation for the Neo-Proterozoic meta-plagiogranites of the NE Jiangxi ophiolitic mélange belt, South China[J]. Lithos, 110: 277-293.

Gao S, Yang J, Zhou L, Li M, Hu Z C, Guo J L, Yuan H L, Gong H, Xiao G H, Wei J Q. 2011. Age and growth of the Archean Kongling terrain, South China, with emphasis on 3.3 Ga granitoid gneisses[J]. American Journal of Science, 311: 153-182.

Garzanti E, Andò S, France-Lanord C, Vezzoli G, Censi P, Galy V, Najman Y. 2010. Mineralogical and chemical variability of fluvial sediments: 1. Bedload sand (Ganga-Brahmaputra, Bangladesh) [J]. Earth and Planetary Science Letters, 299: 368-381.

Garzanti E, Limonta M, Resentini A, Bandopadhyay P C, Najman Y, Andò S, Vezzoli G. 2013a. Sediment recycling at convergent plate margins (Indo-Burman Ranges and Andaman-Nicobar Ridge) [J]. Earth-Science Reviews, 123: 113-132.

Garzanti E, Padoan M, Andò S, Resentini A, Vezzoli G, Lustrino M. 2013b. Weathering and Relative Durability of Detrital Minerals in Equatorial Climate: Sand Petrology and Geochemistry in the East African Rift[J]. The Journal of Geology, 121: 547-580.

Gehrels G, 2014. Detrital zircon U-Pb geochronology applied to tectonics[J]. Annual Review of Earth and Planetary Sciences, 42: 127-149.

Gehrels G, Rusmore M, Woodsworth G, Crawford M, Andronicos C, Hollister L, Patchett J, Ducea M, Butler R, Klepeis K, Davidson C, Friedman R, Haggart J, Mahoney B, Crawford W, Pearson D, Girardi J. 2009. U-Th-Pb geochronology of the Coast Mountains batholith in north-coastal British Clumbia: Constraints on age and tectonic evolution[J]. Geological Society of America Bulletin, 121: 1341-1361.

Greentree M R, Li Z X. 2008. The oldest known rocks in south-western China: SHRIMP U-Pb magmatic crystallisation age and detrital provenance analysis of the Paleoproterozoic Dahongshan Group[J]. Journal of Asian Earth Sciences, 33: 289-302.

Guo J L, Gao S, Wu Y B, Li M, Chen K, Hu Z C, Liang Z W, Liu Y S, Zhou L, Zong K Q, Zhang W, Chen H H. 2014. 3.45Ga granitic gneisses from the Yangtze Craton, South China: Implications for Early Archean crustal growth[J]. Precambrian Research, 242: 82-95.

Guo J L, Wu Y B, Gao S, Jin Z M, Zong K Q, Hu Z C, Chen K, Chen H H, Liu Y S. 2015. Episodic Paleoarchean-Paleoproterozoic (3.3-2.0 Ga) granitoid magmatismin Yangtze Craton, South China: implications for late Archean tectonics[J]. Precambrian Research, 270: 246-266.

Guo L Z, Shi Y S, Lu H F, Ma R S, Dong H G, Yang S F. 1989. The pre-Devonian tectonic patterns and evolution of South China[J]. Journal of Southeast Asian Earth Sciences, 3: 87-93.

Guo R H, Hu X M, Garzanti E, Lai W, Yan B, Mark C. 2020. How faithfully do the geochronological and geochemical signatures of detrital zircon, titanite, rutile and monazite record magmatic and metamorphic events? A case study from the Himalaya and Tibet[J]. Earth-Science Reviews, 201: 103082.

Guo Y L, Yang S Y, Su N, Li C, Yin P, Wang Z B. 2018. Revisiting the effects of hydrodynamic sorting and sedimentary recycling on chemical weathering indices[J]. Geochimica et Cosmochimica Acta, 227: 48-63.

Hadlari T, Swindles G T, Galloway J M, Bell K M, Sulphur K C, Heaman L M, Beranek L P, Fallas K M. 2015. 1.8 Billion Years of Detrital Zircon Recycling Calibrates a Refractory Part of Earth's Sedimentary Cycle[J]. PLOS ONE, 10: e0144727.

Han P Y, Guo J L, Chen K, Huang H, Zong K Q, Liu Y S, Hu Z C, Gao S. 2017. Widespread Neoarchean (~2.7-2.6Ga) magmatism of the Yangtze craton, South China, as revealed by modern river detrital zircons[J]. Gondwana Research, 42: 1-12.

Han Q S, Peng S B, Polat A, Kusky T, Deng H, Wu T Y. 2018. A ca.2.1 Ga Andean type margin built on metasomatized lithosphere in the northern Yangtze craton,China: evidence from high-Mg basalts and andesites[J]. Precambrian Research, 309: 309-324.

Han Q S, Peng S B, Polat A, Kusky T. 2019. Petrogenesis and geochronology of Paleoproterozoic magmatic rocks in the Kongling complex: Evidence for a collisional orogenic event in the Yangtze craton[J]. Lithos, 342-343: 513-529.

Hawkesworth C J, Dhuime B, Pietranik A B, Cawood P A, Kemp A I S, Storey C D. 2010. The generation and evolution of the continental crust[J]. Journal of Geographical Sciences, 167: 229-248.

Hawkesworth C, Cawood P, Kemp T, Storey C, Dhuime B. 2009. A Matter of Preservation[J]. Science, 323: 49-50.

He M Y, Zheng H B, Bookhagen B, Clift P D. 2014. Controls on erosion intensity in the Yangtze River basin tracked by U-Pb detrital zircon dating[J]. Earth-Science Reviews, 136: 121-140.

He M Y, Zheng H B, Clift P D. 2013. Zircon U-Pb geochronology and Hf isotope data from the Yangtze River sands: Implications for major magmatic events and crustal evolution in Central China[J]. Chemical Geology, 360-361: 186-203.

Holland H D, Gottfried D. 1955. The effect of nuclear radiation on the structure of zircon[J]. Acta Crystallographica, 8: 291-300.

Horne A M, van Soest M C, Hodges K V, Tripathy-Lang A, Hourigan J K. 2016. Integrated single crystal laser ablation U/Pb and （U-Th）/He dating of detrital accessory minerals - Proof-of-concept studies of titanites and zircons from the Fish Canyon tuff[J]. Geochimica et Cosmochimica Acta, 178: 106-123.

Hoskin P W O, Ireland T R. 2000. Rare earth element chemistry of zircon and its use as a provenance indicator[J]. Geology 28：627-630.

Hu J, Liu X C, Chen L Y, Qu W, Li H K, Geng J Z. 2013. A ~ 2.5 Ga magmatic event at the northern margin of the Yangtze craton: Evidence from U-Pb dating and Hf isotope analysis of zircons from the Douling Complex in the South Qinling orogen[J]. Chinese Science Bulletin, 58: 3564-3579.

Hui B, Dong Y P, Cheng C, Long X P, Liu X, Yang Z, Sun S S, Zhan F F, Varga J. 2017. Zircon U-Pb chronology, Hf isotope analysis and whole-rock geochemistry for the Neoarchean-Paleoproterozoic Yudongzi complex, northwestern margin of the Yangtze craton, China[J]. Precambrian Research, 301: 65-85.

Iizuka T, Komiya T, Rino S, Maruyama S, Hirata T. 2010. Detrital zircon evidence for Hf isotopic evolution of granitoid crust and continental growth[J]. Geochimica et Cosmochimica Acta, 74: 2450-2472.

Iizuka T, Campbell I H, Allen C M, Gill J B, Maruyama S, Makoka F, 2013. Evolution of the African continental crust as recorded by U-Pb, Lu-Hf and O isotopes in detrital zircons from modern rivers. Geochimica et Cosmochimica Acta, 107: 96-120.

Jäger H. 2004. Facies dependence of spore assemblages and new data on sedimentary influence on spore taphonomy[J]. Review of Palaeobotany and Palynology, 130: 121-140.

Jiang S H, Nie F J, Fang D, Liu Y. 2009. Geochronology and Geochemical Features of the Main Intrusive Rocks in Weishancheng Area, Tongbai county, Henan[J]. Acta Geologica Sinica, 83: 1011-1029.

Jiang W C, Li H, Mathur R , Wu J H. 2019. Genesis of the giant Shizhuyuan W-Sn-Mo-Bi-Pb-Zn polymetallic deposit, South China: Constraints from zircon geochronology and geochemistry in skarns[J]. Ore Geology Reviews, 111: 102980.

Jiao W F, Wu Y B, Yang S H, Peng M, Wang J. 2009. The oldest basement rock in the Yangtze Craton revealed by zircon U-Pb age and Hf isotope composition[J]. Science in China Series D: Earth Science, 52: 1393-1399.

Kuenen P H. 1959. Experimental abrasion 3. Fluviatile action on sand[J]. American Journal of Science, 257: 172-190.

Li H, Zhang C L, Xiang Z Q, Lu S N, Jian Z, Geng J Z, Qu L S, Wang Z X. 2013. Zircon and baddeleyite U-Pb geochronology of the Shennongjia Group in the Yangtze Craton and its tectonic significance[J]. Acta Petrologica Sinica, 29: 673-697.

Li W X, Li X H, Li Z X. 2005. Neoproterozoic bimodal magmatism in the Cathaysia Block of South China and its tectonic significance[J]. Precambrian Research, 136: 51-66.

Li X H, Li W X, Li Z X, Lo C H, Wang J, Ye M F, Yang Y H. 2009. Amalgamation between the Yangtze and Cathaysia Blocks in South China: Constraints from SHRIMP U-Pb zircon ages, geochemistry and Nd-Hf isotopes of the Shuangxiwu volcanic rocks[J]. Precambrian Research, 174: 117-128.

Li X H, Li Z X, Ge W, Zhou H, Li W, Liu Y, Wingate M T D. 2003. Neoproterozoic granitoids in South China: crustal melting above a mantle plume at ca. 825 Ma? [J] Precambrian Research, 122: 45-83.

Li X H, Zhou G Q, Zhao J X, Fanning C M, Compston W. 1994. SHRIMP ion microprobe zircon U-Pb Age and Sm-Nd isotopic characteristics of the NE Jiangxi ophiolite and its tectonic implications[J]. Chinese Journal of Geochemistry, 13: 317-325.

Li X H. 1999. U-Pb zircon ages of granites from the southern margin of the Yangtze Block: timing of Neoproterozoic Jinning: Orogeny in SE China and implications for Rodinia Assembly[J]. Precambrian Research, 97: 43-57.

Li Z X, Li X, Zhou H, Kinny P D. 2002. Grenvillian continental collision in south China: New SHRIMP U-Pb zircon results and implications for the configuration of Rodinia[J]. Geology, 30: 163-166.

Liang Z W, Gao S, Hawkesworth C J, Wu Y B, Storey C D, Zhou L, Li M, Hu Z C, Liu Y S, Liu X M. 2018. Step-like growth of the continental crust in South China: evidence from detrital zircons in Yangtze River sediments[J]. Lithos, 320-321: 155-171.

Liu B, Zhai M G, Zhao L, Cui X H, Zhou L G. 2019. Zircon U-Pb-Hf isotope studies of the early Precambrian metasedimentary rocks in the Kongling terrane of the Yangtze Block, South China[J]. Precambrian Research, 320: 334-349.

Liu Q, Yu J H, O'Reilly S Y, Zhou M F, Griffin W L, Wang L, Cui X. 2014. Origin and geological significance of Paleoproterozoic granites in the northeastern Cathaysia Block, South China[J]. Precambrian Research, 248: 72-95.

Liu X C, Wu Y B, Fisher C M, Hanchar J M, Beranek L, Gao S, Wang H. 2017. Tracing crustal evolution by U-Th-Pb, Sm-Nd, and Lu-Hf isotopes in detrital monazite and zircon from modern rivers[J]. Geology, 45: 103-106.

Mehring J L, McBride E F. 2007. Origin of modern quartzarenite beach sands in a temperate climate, Florida and Alabama, USA[J]. Sedimentary Geology, 201: 432-445.

Meng L, Li Z X, Chen H, Li X H, Zhu C. 2015. Detrital zircon U-Pb geochronology, Hf isotopes and geochemistry constraints on crustal growth and Mesozoic tectonics of southeastern China[J]. Journal of Asian Earth Sciences, 105: 286-299.

Mezger K, Krogstad E J. 1997. Interpretation of discordant U-Pb zircon ages: An evaluation[J]. Journal of Metamorphic Geology, 15: 127-140.

Moecher D P, Kelly E A, Hietpas J, Samson S D. 2019. Proof of recycling in clastic sedimentary systems from textural analysis and geochronology of detrital monazite: Implications for detrital mineral provenance analysis[J]. Geological Society of America Bulletin, 131: 1115-1132.

Moecher D P, Samson S D. 2006. Differential zircon fertility of source terranes and natural bias in the detrital zircon record: Implications for sedimentary provenance analysis[J]. Earth and Planetary Scienc Letters, 247: 252-266.

Moecher D P, Zotto S C, Samson S D. 2023. The critical role of recycling of post-Grenvillian, Neoproterozoic sediments for Phanerozoic Laurentian clastic systems: evidence from detrital-zircon and -monazite geochronology and textures[J]. Journal of Sedimentary Research, 93: 118-144.

Murakami T, Chakoumakos B, Ewing R, Lumpkin G, Weber W. 1991. Alpha-Decay Event Damage in Zircon[J]. American Mineralogist, 76:9-10.

Nasdala L, Wenzel M, Vavra G, Irmer G, Wenzel T, Kober, B. 2001. Metamictisation of natural zircon: accumulation versus thermal annealing of radioactivity-induced damage[J]. Contributions to Mineralogy and Petrology, 141: 125-144.

Nie H, Yang J Z, Zhou G Y, Liu C Z, Zheng J P, Zhang W X, Zhao Y J, Wang H, Wu Y B. 2017. Geochemical and Re-Os isotope constraints on the origin and age of the Songshugou peridotite massif in the Qinling orogen, central China[J]. Lithos, 292-293: 307-319.

Parman S W. 2015. Time-lapse zirconography: Imaging punctuated continental evolution[J]. Geochemical Perspectives Letters, 43-52.

Pell S D, Williams I S, Chivas A R, 1997. The use of protolith zircon-age fingerprints in determining the protosource areas for some Australian dune sands[J]. Sedimentary Geology, 109: 233-260.

Peng S B, Kusky T M, Jiang X F, Wang L, Wang J P, Deng H. 2012. Geology, geochemistry, and geochronology of the Miaowan ophiolite, Yangtze craton: Implications for South China's amalgamation history with the Rodinian supercontinent[J]. Gondwana Research, 21: 577-594.

Peters S E, Husson J M. 2017. Sediment cycling on continental and oceanic crust[J]. Geology, 45: 323-326.

Peters S E, Walton C R, Husson J M, Quinn D P, Shorttle O, Keller C B, Gaines R R. 2021. Igneous rock area and age in continental crust[J]. Geology, 49: 1235-1239.

Pietranik A B, Hawkesworth C J, Storey C D, Kemp A I S, Sircombe K N, Whitehouse M J, Bleeker W. 2008. Episodic, mafic crust formation from 4.5 to 2.8 Ga: New evidence from detrital zircons, Slave craton, Canada[J]. Geological, 36: 875-878.

Puetz S J. 2018. A relational database of global U-Pb ages[J]. Geoscience Frontiers, 9: 877-891.

Pullen A, Ibáñez-Mejía M, Gehrels G E, Ibáñez-Mejía J C, Pecha M. 2014. What happens when n= 1000? Creating large-n geochronological datasets with LA-ICP-MS for geologic investigations[J]. Journal of Analytical Atomic Spectrometry, 29(6): 971-980.

Pullen A, Kapp P, Gehrels G E, Ding L, Zhang Q. 2011. Metamorphic rocks in central Tibet: Lateral variations and implications for crustal structure[J]. Geological Society of America Bulletin, 123: 585-600.

Rasmussen B, Fletcher I R, Muhling J R. 2007. In situ U-Pb dating and element mapping of three generations of monazite: Unravelling cryptic tectonothermal events in low-grade terranes[J]. Geochimica et Cosmochimica Acta, 71: 670-690.

Reiners P W, Campbell I H, Nicolescu S, Allen C M, Hourigan J K, Garver J I, Mattinson J M, Cowan D S. 2005. (U-Th)/(He-Pb) double dating of detrital zircons[J]. American Journal of Science, 305: 259-311.

Roberts N M W, Spencer C J. 2015. The zircon archive of continent formation through time[A].//Roberts N M W, Van Kranendonk M, Parman S, Shirey S, Clift P D. 2015. Continent Formation Through Time. Geological Society, London, Special Publications, 389: 197-225.

Roser B P, Korsch R J. 1999. Geochemical characterization, evolution and source of a Mesozoic accretionary wedge: the Torlesse terrane, New Zealand[J]. Geological Magazine, 136: 493-512.

Samson S D, Moecher D P, Satkoski A M. 2018. Inherited, enriched, heated, or recycled? Examining potential causes of Earth's most zircon fertile magmatic episode[J]. Lithos, 314-315: 350-359.

Shaanan U, Rosenbaum G. 2018. Detrital zircons as palaeodrainage indicators: insights into southeastern Gondwana from Permian basins in eastern Australia[J]. Basin Research, 30: 36-47.

Sharman G R, Malkowski M A. 2020. Needles in a haystack: Detrital zircon U-Pb ages and the maximum depositional age of modern global sediment[J]. Earth-Science Reviews, 203: 103109.

Shu L S, Deng P, Yu J H, Wang Y B, Jiang S Y. 2008a. The age and tectonic environment of the rhyolitic rocks on the western side of Wuyi Mountain, South China[J]. Science in China Series D: Earth Science, 51: 1053-1063.

Shu L S, Faure M, Jiang S Y, Yang Q, Wang Y. 2006. SHRIMP zircon U-Pb age, litho- and biostratigraphic analyses of the Huaiyu Domain in South China[J]. Episodes, 29: 244-252.

Shu L S, Faure M, Wang B, Zhou X M, Song B. 2008b. Late Palaeozoic-Early Mesozoic geological features of South China: Response to the Indosinian collision events in Southeast Asia[J]. Comptes Rendus Géoscience, 340: 151-165.

Shu L S, Faure M, Yu J H, Jahn B M. 2011. Geochronological and geochemical features of the Cathaysia block (South China): New evidence for the Neoproterozoic breakup of Rodinia[J]. Precambrian Research, 187: 263-276.

Shu L S, Charvet J. 1996. Kinematics and geochronology of the Proterozoic Dongxiang-Shexian ductile shear zone: with HP metamorphism and ophiolitic melange (Jiangnan Region, South China) [J]. Tectonophysics, 267: 291-302.

Shukri. 1949. The mineralogy of some nile sediments[J]. Quarterly Journal of the Geological Society, 105: 511-534.

Song F, Niu Z J, He Y Y, Algeo T J, Yang W Q. 2020. Geographic proximity of Yangtze and Cathaysia blocks during the late Neoproterozoic demonstrated by detrital zircon evidence[J]. Palaeogeography, Palaeoclimatology, Palaeoecology, 558: 109939.

Spencer C J, Kirkland C L, Roberts N M W. 2018. Implications of erosion and bedrock composition on zircon fertility: Examples from South America and Western Australia[J]. Terra Nova，30：289-295.

Steiger R H, Jäger E. 1977. Subcommission on geochronology: Convention on the use of decay constants in geo- and cosmochronology[J]. Earth and Planetary Science Letters，36: 359-362.

Stevens T, Carter A, Watson T P, Vermeesch P, Andò S, Bird A F, Lu H, Garzanti E, Cottam M A, Sevastjanova I. 2013. Genetic linkage between the Yellow River, the Mu Us desert and the Chinese Loess Plateau[J]. Quaternary Science Reviews, 78: 355-368.

Voice P J, Kowalewsk, M, Eriksson K A. 2011. Quantifying the Timing and Rate of Crustal Evolution: Global Compilation of Radiometrically Dated Detrital Zircon Grains[J]. The Journal of Geology, 119: 109-126.

Wang B Q, Wang W, Chen W T, Gao J F, Zhao X F, Yan D P, Zhou M F. 2013. Constraints of detrital zircon U-Pb ages and Hf isotopes on the provenance of the Triassic Yidun Group and tectonic evolution of the Yidun Terrane, Eastern Tibet[J]. Sedimentary Geology, 289: 74-98.

Wang D Z, Zhou X M, Xu X S. 1989. Types and genetic model of Precambrian granitoids of South China[J]. Journal of Southeast Asian Earth Sciences, 3: 255-261.

Wang K, Dong S W, Li Z X, Han B F. 2018a. Age and chemical composition of Archean metapelites in the Zhongxiang Complex and implications for early crustal evolution of the Yangtze Craton[J]. Lithos, 320-321: 280-301.

Wang K, Dong S W. 2019. New insights into Paleoproterozoic tectonics of the Yangtze Block in the context of early Nuna assembly: Possible collisional granitic magmatism in the Zhongxiang Complex, South China[J]. Precambrian Research, 334: 105452.

Wang K, Li Z X, Dong S W, Cui J J, Han B F, Zheng T, Xu Y L. 2018b. Early crustal evolution of the Yangtze Craton, South China: New constraints from zircon U-Pb-Hf isotopes and geochemistry of ca. 2.9-2.6 Ga granitic rocks in the Zhongxiang Complex[J]. Precambrian Research, 314: 325-352.

Wang L J, Griffin W L, Yu J H, O'Reilly S Y. 2013. U-Pb and Lu-Hf isotopes in detrital zircon from Neoproterozoic sedimentary rocks in the northern Yangtze Block: Implications for Precambrian crustal evolution[J]. Gondwana Research, 23: 1261-1272.

Wang T, Wang X X, Tian W, Zhang C L, Li W P, Li S. 2009. North Qinling Paleozoic granite associations and their variation in space and time: Implications for orogenic processes in the orogens of central China[J]. Science in China Series D: Earth Sciences, 52: 1359-1384.

Wang W, Cawood P A, Zhou M F, Zhao J H. 2016. Paleoproterozoic magmatic and metamorphic events link Yangtze to northwest Laurentia in the Nuna supercontinent[J]. Earth and Planetary Science Letters 433: 269-279.

Wang W, Wang F, Chen F K, Zhu X Y, Xiao P, Siebel W. 2010. Detrital Zircon Ages and Hf-Nd Isotopic Composition of Neoproterozoic Sedimentary Rocks in the Yangtze Block: Constraints on the Deposition Age and Provenance[J]. The Journal of Geology, 118: 79-94.

Wang W, Zhou M F, Zhao X F, Chen W T, Yan D P. 2014. Late Paleoproterozoic to Mesoproterozoic rift successions in SW China: Implication for the Yangtze Block-North Australia-Northwest Laurentia connection in the Columbia supercontinent[J]. Sedimentary Geology, 309: 33-47.

Wang W, Zhou M F. 2014. Provenance and tectonic setting of the Paleo- to Mesoproterozoic Dongchuan Group in the southwestern Yangtze Block, South China: Implication for the breakup of the supercontinent Columbia[J]. Tectonophysics, 610: 110-127.

Wang X L, Zhou J C, Qiu J S, Zhang W L, Liu X M, Zhang G L. 2006. LA-ICP-MS U-Pb zircon geochronology of the Neoproterozoic igneous rocks from Northern Guangxi, South China: Implications for tectonic evolution[J]. Precambrian Research, 145: 111-130.

Wang Y J, Zhang A M, Cawood P A, Fan W M, Xu J F, Zhang G W, Zhang Y Z. 2013. Geochronological, geochemical and Nd-Hf-Os isotopic fingerprinting of an early Neoproterozoic arc-back-arc system in South China and its accretionary assembly along the margin of Rodinia[J]. Precambrian Research, 231: 343-371.

Wang Z J, Wang J, Deng Q, Du Q D, Zhou X L, Yang F, Liu H. 2015. Paleoproterozoic I-type granites and their implications for the Yangtze block position in the Columbia supercontinent: Evidence from the Lengshui Complex, South China[J]. Precambrian Research, 263: 157-173.

Wang Z J, Wang J, Du Q D, Deng Q, Yang F, Wu H. 2013. Mature Archean continental crust in the Yangtze craton: Evidence from petrology, geochronology and geochemistry[J]. Chinese Science Bulletin, 58: 2360-2369.

Wei Y X, Zhou W X, Hu Z X, Li H Q, Huang X X, Zhao X M, Xu D X. 2019. Geochronology and Geochemistry of Archean TTG and Tremolite Schist Xenoliths in Yemadong Complex: Evidence for ≥3.0 Ga Archean Continental Crust in Kongling High-Grade Metamorphic Terrane, Yangtze Craton, China[J]. Minerals, 9: 689.

Weislogel A L, Graham S A, Chang E Z, Wooden J L, Gehrels G E, Yang H. 2006. Detrital zircon provenance of the Late Triassic Songpan-Ganzi complex: Sedimentary record of collision of the North and South China blocks[J]. Geology, 34: 97-100.

Wilde S A, Valley J W, Peck W H, Graham C M. 2001. Evidence from detrital zircons for the existence of continental crust and oceans on the Earth 4.4 Gyr ago[J]. Nature, 409: 175-178.

Wilkinson B H, McElroy B J, Kesler S E, Peters S E, Rothman E D. 2009. Global geologic maps are tectonic speedometers--Rates of rock cycling from area-age frequencies[J]. Geological Society of America Bulletin, 121: 760-779.

Wissink G K, Hoke G D. 2016. Eastern margin of Tibet supplies most sediment to the Yangtze River[J]. Lithosphere, 8: 601-614.

Wu Y B, Gao S, Zhang H F, Zheng J P, Liu X C, Wang H, Gong H J, Zhou L, Yuan H L. 2012. Geochemistry and zircon U-Pb geochronology of Paleoproterozoic arc related granitoid in the Northwestern Yangtze Block and its geological implications[J]. Precambrian Research, 200-203: 26-37.

Wu Y B, Zheng Y F. 2013. Tectonic evolution of a composite collision orogen: An overview on the Qinling-Tongbai-Hong'an-Dabie-Sulu orogenic belt in central China[J]. Gondwana Research, 23: 1402-1428.

Wu Y B, Zhou G Y, Gao S, Liu X C, Qin Z W, Wang H, Yang J Z, Yang S H. 2014. Petrogenesis of Neoarchean TTG rocks in the Yangtze Craton and its implication for the formation of Archean TTGs[J]. Precambrian Research, 254: 73-86.

Xiong Q, Zheng J P, Yu C M, Su Y P, Tang H Y, Zhang Z H. 2009. Zircon U-Pb age and Hf isotope of Quanyishang A-type granite in Yichang: signification for the Yangtze continental cratonization in Paleoproterozoic[J]. Chinese Science Bulletin, 54: 436-446.

Xu D L, Wei Y X, Peng L H, Deng, X, Hu K, Liu H. 2018. A ca. 2.2Ga Acidic Magmatic Event at the Northern Margin of the Yangtze Craton: Evidence from U-Pb Dating and Hf Isotope Analysis of Zircons from the Kongling Complex[J]. Acta Geologica Sinica - English Edition, 92: 872-873.

Xu J, Stockli D F, Snedden J W. 2017. Enhanced provenance interpretation using combined U-Pb and (U-Th)/He double dating of detrital zircon grains from lower Miocene strata, proximal Gulf of Mexico Basin, North America[J]. Earth and Planetary Science Letters, 475: 44-57.

Yang C, Li X H, Wang X C, Lan Z. 2015. Mid-Neoproterozoic angular unconformity in the Yangtze Block revisited: Insights from detrital zircon U-Pb age and Hf-O isotopes[J]. Precambrian Research, 266: 165-178.

Yang S Y, Zhang F, Wang Z B. 2012. Grain size distribution and age population of detrital zircons from the Changjiang (Yangtze) River system, China[J]. Chemical Geology, 296-297: 26-38.

Yang Z N, Yang K G, Polat A, Xu Y. 2018. Early crustal evolution of the eastern Yangtze Block: Evidence from detrital zircon U-Pb ages and Hf isotopic composition of the Neoproterozoic Huashan Group in the Dahongshan area[J]. Precambrian Research, 309: 248-270.

Yao J L, Shu L S, Santosh M, Li J Y. 2012. Precambrian crustal evolution of the South China Block and its relation to supercontinent history: Constraints from U-Pb ages, Lu-Hf isotopes and REE geochemistry of zircons from sandstones and granodiorite[J]. Precambrian Research, 208-211: 19-48.

Ye M F, Li X H, Li W X, Liu Y, Li Z X. 2007. SHRIMP zircon U-Pb geochronological and whole-rock geochemical evidence for an early Neoproterozoic Sibaoan magmatic arc along the southeastern margin of the Yangtze Block[J]. Gondwana Research, 12: 144-156.

Yin C Y, Lin S F, Davis D W, Zhao G C, Xiao W J, Li L M, He Y H. 2013. 2.1-1.85Ga tectonic events in the Yangtze Block, South China: Petrological and geochronological evidence from the Kongling Complex and implications for the reconstruction of supercontinent Columbia[J]. Lithos, 182-183: 200-210.

Yu J H, Wang L J, O'Reilly S Y, Griffin W L, Zhang M, Li C Z, Shu L S. 2009. A Paleoproterozoic orogeny recorded in a long-lived cratonic remnant (Wuyishan terrane), eastern Cathaysia Block, China[J]. Precambrian Research, 174: 347-363.

Zhang L J, Ma C Q, Wang L X, She Z B, Wang S M. 2011. Discovery of Paleoproterozoic rapakivi granite on the northern margin of the Yangtze block and its geological significance[J]. Chinese Science Bulletin, 56: 306-318.

Zhang M, Salje E K H, Capitani G C, Leroux H, Clark A M, Schlüter J, Ewing R C. 2000. Annealing of -decay damage in zircon: a Raman spectroscopic study[J]. Journal of Physics: Condensed Matter, 12: 3131.

Zhang S B, Zheng Y F, Wu P, He Q, Rong W, Fu B, Yang Y H, Liang T. 2020. The nature of subduction system in the Neoarchean: Magmatic records from the northern Yangtze Craton, South China[J]. Precambrian Research, 347: 105834.

Zhang S B, Zheng Y F, Wu Y B, Zhao Z F, Gao S, Wu F Y. 2006. Zircon U-Pb age and Hf-O isotope evidence for Paleoproterozoic metamorphic event in South China[J]. Precambrian Research, 151: 265-288.

Zhao G C, Cawood P A. 2012. Precambrian geology of China[J]. Precambrian Research, 222-223: 13-54.

Zhao L, Zhou X W, Zhai M G, Santosh M, Ma X D, Shan H X, Cui X H. 2014. Paleoproterozoic tectonic transition from collision to extension in the eastern Cathaysia Block, South China: Evidence from geochemistry, zircon U-Pb geochronology and Nd-Hf isotopes of a granite-charnockite suite in southwestern Zhejiang[J]. Lithos, 184-187: 259-280.

Zhao T, Zhu G, Wu Q, Hu R M, Wu Y H, Xu Z Y, Ye J. 2021. Evidence for discrete Archean microcontinents in the Yangtze Craton[J]. Precambrian Research, 361: 106259.

Zhong N, Song X S, Xu H Y, Jiang H C. 2017. Influence of a tectonically active mountain belt on its foreland basin: Evidence from detrital zircon dating of bedrocks and sediments from the eastern Tibetan Plateau and Sichuan Basin, SW China[J]. Journal of Asian Earth Sciences, 146: 251-264.

Zhou G Q, Zou H B. 1996. Precambrian High-Pressure Metamorphic Rocks within the Collision Zone of the Yangtze and Cathaysia Blocks, China: Jadeite/Glaucophane-Type Facies[J]. International Geology Review, 38: 87-93.

Zhou G Y, Fisher C M, Luo Y, Pearson D G, Li L, He Y, Wu Y B. 2020. A clearer view of crustal evolution: U-Pb, Sm-Nd, and Lu-Hf isotope systematics in five detrital minerals unravel the tectonothermal history of northern China[J]. Geological Society of America Bulletin, 132: 2367-2381.

Zhou G Y, Wu Y B, Gao S, Yang J, Zheng J P, Qin Z W, Wang H, Yang S H. 2015. The 2.65 Ga A-type granite in the northeastern Yangtze craton: Petrogenesis and geological implications[J]. Precambrian Research, 258: 247-259.

Zhou G Y, Wu Y B, Li L, Zhang W X, Zheng J P, Wang H, Yang S H. 2018. Identification of ca. 2.65 Ga TTGs in the Yudongzi complex and its implications for the early evolution of the Yangtze Block[J]. Precambrian Research, 314: 240-263.

Zhou G Y, Wu Y B, Wang H, Qin Z, Zhang W X, Zheng J P, Yang S H. 2017. Petrogenesis of the Huashanguan A-type granite complex and its implications for the early evolution of the Yangtze Block[J]. Precambrian Research, 292: 57-74.

Zhu Z Y, Campbell I H, Allen C M, Li Z, 2023. Evolution of the preserved European continental crust, constrained by U-Pb, O and Hf isotopic analyses of river detrital zircons[J]. Geochimica et Cosmochimica Acta, 346: 133-148.

Zieger J, Rothe J, Hofmann M, Gärtner A, Linnemann U. 2019. The Permo-Carboniferous Dwyka Group of the Aranos Basin（Namibia）- How detrital zircons help understanding sedimentary recycling during a major glaciation[J]. Journal of African Earth Sciences, 58: 103555.

Zoleikhaei Y, Mulder J A, Cawood P A. 2021. Integrated detrital rutile and zircon provenance reveals multiple sources for Cambrian sandstones in North Gondwana[J]. Earth-Science Reviews, 213: 103462.

Zoleikhaei Y, Mulder J A, Cawood P A. 2022. Evaluating sediment recycling through combining inherited petrogenic and acquired sedimentary features of multiple detrital minerals[J]. Basin Research, 34: 1055-1083.

Zotto S C, Moecher D P, Niemi N A, Thigpen J R, Samson S D. 2020. Persistence of Grenvillian dominance in Laurentian detrital zircon age systematics explained by sedimentary recycling: Evidence from detrital zircon double dating and detrital monzite textures and geochronology[J]. Geology, 48: 792-797.